Supplementary Material Available: A listing of observed and calculated structure factors and a table of positional and thermal parameters (32 pages). Ordering information is given on any current masthead page.

References and Notes

(1) (a) Tetracarbon Metallocarboranes. 8. (b) For part 7, see W. M. Maxwell and R. N. Grimes, *Inorg. Chem.*, in press.
(2) W. N. Lipscomb, "Boron Hydrides", W. A. Benjamin, New York, 1963, and references cited therein.
(3) H. C. Longuet-Higgins and M. de V. Roberts, *Proc. R. Soc. London, Ser. A*, **224**, 336 (1954); **230**, 110 (1955).
(4) E. B. Moore, Jr., L. L. Lohr, Jr., and W. N. Lipscomb, *J. Chem. Phys.*, **35**, 1329 (1961).
(5) Procedures for counting framework electrons in polyhedral cages are given by (a) K. Wade, *Adv. Inorg. Chem. Radiochem.*, **18**, 1 (1976); (b) D. M. P. Mingos, *Nature (London), Phys. Sci.*, **236**, 99 (1972); (c) R. W. Rudolph, *Acc. Chem. Res.*, **9**, 446 (1976).
(6) M. R. Churchill and B. G. DeBoer, *Inorg. Chem.*, **12**, 2674 (1973).
(7) E. I. Tolpin and W. N. Lipscomb, *Inorg. Chem.*, **12**, 2257 (1973).
(8) D. P. Freyberg, R. Weiss, E. Sinn, and R. N. Grimes, *Inorg. Chem.*, **16**, 1847 (1977).
(9) W. M. Maxwell, R. F. Bryan, and R. N. Grimes, *J. Am. Chem. Soc.*, **99**, 4008 (1977).
(10) K-S. Wong, J. R. Bowser, J. R. Pipal, and R. N. Grimes, *J. Am. Chem. Soc.*, **100**, 5045 (1978).
(11) J. R. Pipal and R. N. Grimes, *Inorg. Chem.*, in press.
(12) J. R. Pipal and R. N. Grimes, *J. Am. Chem. Soc.*, **100**, 3083 (1978).
(13) E. Sinn, J. R. Pipal, and R. N. Grimes, to be submitted for publication.
(14) R. E. Williams, *Inorg. Chem.*, **10**, 210 (1971).
(15) P. W. R. Corfield, R. J. Doedens, and J. A. Ibers, *Inorg. Chem.*, **6**, 197 (1967).
(16) D. T. Cromer and J. T. Waber, "International Tables for X-ray Crystallography", Vol. IV, Kynoch Press, Birmingham, England, 1974.
(17) R. F. Stewart, E. R. Davidson, and W. T. Simpson, *J. Chem. Phys.*, **42**, 3175 (1965).
(18) D. T. Cromer and J. A. Ibers, ref. 16.
(19) D. P. Freyberg, G. M. Mockler, and E. Sinn, *J. Chem. Soc., Dalton Trans.*, 447 (1976).
(20) Nido cages contain 2n + 4 skeletal electrons (where n is the number of framework atoms) and normally adopt open geometry based on a closed polyhedral (closo) cage with one missing vertex. Arachno systems have 2n + 6 skeletal electrons and resemble closo polyhedra with two missing vertices.[5,14]
(21) The prototype closo 14-vertex polyhedron is a bicapped hexagonal antiprism, of which the only structurally established example is $(\eta^5\text{-}C_5H_5)_2Fe_2(CH_3)_4C_4B_8H_8$ (isomer VIII).[22,23]
(22) J. R. Pipal and R. N. Grimes, *Inorg. Chem.*, **17**, 6 (1978).
(23) W. M. Maxwell, R. Weiss, E. Sinn, and R. N. Grimes, *J. Am. Chem. Soc.*, **99**, 4016 (1977).
(24) Early structural proposals,[25] made prior to the crystallographic studies, speculated that A and B had open and closed geometries, respectively. Subsequently, the observed[8] structure of A turned out to be very similar to that originally proposed for B.
(25) W. M. Maxwell, V. R. Miller, and R. N. Grimes, *Inorg. Chem.*, **15**, 1343 (1976).
(26) It is assumed that the cobaltocenium group does not appreciably influence the observed geometry of the carborane anion.
(27) W. N. Lipscomb, *Science*, **153**, 373 (1966).
(28) A neutral $(\eta^5\text{-}C_5H_5)Co(CH_3)_4C_4B_8H_8$ species which is isoelectronic with **4** has been isolated and characterized from the reaction of $CoCl_2$ and NaC_5H_5: see ref 1b.
(29) E. Sinn and R. N. Grimes, to be submitted for publication.

Blue Copper Proteins. Synthesis, Chemistry, and Spectroscopy of $Cu^{I}N_3(SR)$ and $Cu^{II}N_3(SR)$ Active Site Approximations. Crystal Structure of Potassium *p*-Nitrobenzenethiolato(hydrotris(3,5-dimethyl-1-pyrazolyl)borato)cuprate(I) Diacetone, $K[Cu(HB(3,5\text{-}Me_2pz)_3)(SC_6H_4NO_2)]\cdot 2C_3H_6O$

Jeffery S. Thompson, Tobin J. Marks,* and James A. Ibers*

Contribution from the Department of Chemistry and the Materials Research Center, Northwestern University, Evanston, Illinois 60201. *Received September 7, 1978*

Abstract: The cuprous complexes $K[Cu(HB(3,5\text{-}Me_2pz)_3)(SR)]$ (SR = *p*-nitrobenzenethiolate or *O*-ethylcysteinate; $HB(3,5\text{-}Me_2pz)_3$ = hydrotris(3,5-dimethyl-1-pyrazolyl)borate) can be prepared by the reaction of Cu(SR) or $[Cu(SR)](ClO_4)$ with $KHB(3,5\text{-}Me_2pz)_3$ at room temperature. The structure of the complex with SR = *p*-nitrobenzenethiolate has been determined by X-ray diffraction methods. The complex crystallizes in the triclinic space group $C_i^1 - P\bar{1}$ with two molecules in a unit cell of dimensions $a = 10.60\ (2)$ Å, $b = 18.17\ (4)$ Å, $c = 10.33\ (4)$ Å, $\alpha = 93.57\ (5)°$, $\beta = 116.20\ (7)°$, and $\gamma = 71.89\ (5)°$. Least-squares refinement of the 117 variables has led to a value of the conventional R index (on F) of 0.092 for 678 independent reflections having $F_o^2 > 3\sigma(F_o^2)$. The geometry about the Cu^I atom, which is coordinated to three nitrogen atoms and one sulfur atom, is trigonally distorted tetrahedral. The cupric complexes $Cu(HB(3,5\text{-}Me_2pz)_3)(SR)$ (SR = *p*-nitrobenzenethiolate or *O*-ethylcysteinate) have been prepared by the reaction of $KHB(3,5\text{-}Me_2pz)_3$ with the corresponding $[Cu(SR)](ClO_4)$ derivatives at −78 °C. UV–visible, laser Raman, and EPR data are used to show that the Cu^{II} complexes have a very similar structure to that of the Cu^I complex characterized by X-ray diffraction methods. The Cu^{II} complex $Cu(HB(3,5\text{-}Me_2pz)_3(OR)$ (OR = *p*-nitrobenzenephenolate, $OC_6H_4NO_2$) was prepared by the reaction of $NaOC_6H_4NO_2\cdot 2H_2O$ with $CuBr(HB(3,5\text{-}Me_2pz)_3$ in tetrahydrofuran at room temperature. The UV–visible, laser Raman, and EPR data for this complex are used in the interpretation of the spectra of the $Cu^IN_3(SR)$ and $Cu^{II}N_3(SR)$ complexes. The spectral properties of the $Cu^{II}N_3(SR)$ complexes are similar to those of the blue (type 1) copper proteins and allow certain definite conclusions to be drawn concerning the origin of the distinctive UV–visible, resonance Raman, and EPR spectral features of the proteins.

A variety of copper-containing proteins, some of which play important roles in electron transport and/or oxidase activity, contain a highly unusual form of copper ion.[1-6] The "blue" or "type 1" binding sites of metalloproteins such as azurin, plastocyanin, stellacyanin, umecyanin, cytochrome oxidase, ascorbate oxidase, laccase, and ceruloplasmin confer upon the copper ion chemical and spectral properties that are unique among copper complexes.[1-6] These properties include generally high redox potentials compared with the Cu^{II}/Cu^I couple in aqueous solution (i.e., the cuprous form of the type 1 core is unsually stable) and distinctive spectral features. The oxidized, cupric forms of the type 1 proteins display very in-

0002-7863/79/1501-4180$01.00/0

tense optical absorption in the 600-nm region (ϵ 3500–5000 M^{-1} cm^{-1}) and small copper hyperfine coupling in the EPR spectra ($A_{\parallel}$ = 3.3–9.0 × 10^{-3} cm^{-1}).[1-6] The structure of the blue active site has been probed by many chemical and physicochemical techniques. On the basis of chemical,[7] amino acid sequence,[8] cobalt[9] and nickel[10] substitution, kinetic,[11] resonance Raman,[12] CW[13] and pulsed[14] EPR, carbon[15] and proton[15c,16] NMR, infrared spectral,[17] electronic spectral,[18] circular dichroism and magnetic circular dichroism,[18d,19a] EXAFS,[19b] and X-ray photoelectron spectral studies,[20] two basic structural models have been proposed for the blue, type 1 active site (A and B).[8b,12,21] Both models have emphasized that, in

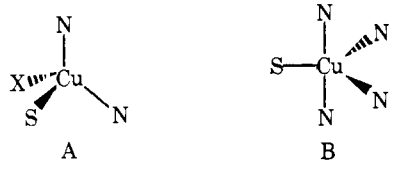

A B

most cases, two of the coordinated nitrogen atoms are from imidazole groups of histidine residues and that one sulfur atom is from a cysteinate mercaptide functionality. Among the proposed four-coordinate (A) structures are those where X is a nitrogen atom of a deprotonated peptide amide, a thioether sulfur atom of a methionine, or an oxygen atom of a tyrosine phenolate.[8b,12,22] That there may not be a unique structure for all type 1 sites is suggested by significant differences among the various proteins in redox potentials, amino acid content, and chemical evidence for copper ligands, as well as in electronic, EPR, and resonance Raman spectra. To what degree the differences in these properties reflect variations in copper ion coordination geometry or actual differences in the ligation sphere, i.e., in the identity of ligand X in structure A, remains to be elucidated.

A recent and very important development in the structural chemistry of the blue copper proteins has been the elucidation, by single-crystal X-ray diffraction methods, of the structure of Cu^{II} poplar (*Populus nigra* Var. *italica*) plastocyanin to 2.7-Å resolution.[23] The results are consistent with structure A in which copper is bound to two histidine imidazole groups as well as a cysteinate sulfur atom, and where X is a methionine thioether sulfur atom. The coordination geometry about the Cu^{II} ion appears to be, at the present stage of refinement, distorted tetrahedral. Furthermore, the copper environment in *Pseudomonas aeruginosa* azurin at 3-Å resolution appears to be rather similar.[24] Considerations of homology suggest that other plastocyanins and azurins have very much the same structure; this conclusion is also in accord with the bulk of the spectra data.[1-6] It is not clear, however, to what degree the structures of other type 1 proteins deviate from the plastocyanin configuration. Certainly, since stellacyanin does not contain methionine,[8c-e] the coordination geometry about the Cu atom must differ from that in poplar plastocyanin.

The above spectral and diffraction studies have added considerably to our understanding of the properties of the blue copper proteins and the structure of the type 1 core. Still, many old questions remain to be answered and a number of new ones have arisen. From an inorganic chemical standpoint, little is known about the chemical and physicochemical characteristics of copper ions in nonclassical binding environments such as in $CuN_2X(SR)$. How the characteristics of such unprecedented species respond to modifications of the ligation sphere is of fundamental importance in understanding chemical, spectrochemical, and structure/function relationships among the type 1 proteins. Few strong connections exist between the mass of protein data and copper complexes of well-characterized structure and behavior. Furthermore, the great bulk of the available physical data on the type 1 proteins deals with the spectroscopically rich Cu^{II} (oxidized) forms. Sparse data are available on the Cu^{I} (reduced) forms that represent the equally important other half of the redox couples.

An informative perspective on the chemical and spectral properties of the native type 1 systems could be provided by parallel studies of simple, low molecular weight synthetic analogues. Such representations, embodying the essential features of the blue copper core, would allow directions of experimentation and modification that are not possible with a molecule as complex and as fragile as a metalloprotein. Recent activity in this area has produced a wealth of interesting new chemistry; however, the compounds generated have been largely ill defined in terms of composition and structure,[25] or, in several instances, possess physiologically implausible ligands and/or biologically unrealistic polymetallic structures.[26] In this contribution we discuss in detail the synthesis, chemistry, spectroscopy, and structures of cuprous and cupric coordination complexes having geometry A where X is a heterocyclic nitrogenous base. A preliminary communication of this work has appeared.[27] We have previously employed the hydrotris(1-pyrazolyl)borate, C ($HBpz_3^-$), and hydrotris(3,5-dimethyl-

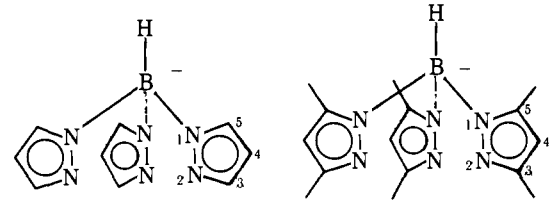

C D

1-pyrazolyl)borate, D ($HB(3,5\text{-}Me_2pz)_3^-$), ligands to approximate polyimidazole binding environments in proteins, such as hemocyanin.[28] In the present work we have utilized D in the assembly of Cu^{I} and Cu^{II} complexes of structure E.

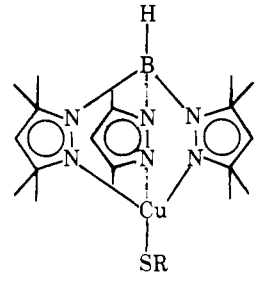

E

These complexes constitute the only well-defined, mononuclear redox pairs to date that approximate any of the proposed type 1 active sites and that, in addition, exhibit many of the unusual spectral properties of the blue copper proteins. Taken together with work on an analogous phenoxide of structure F and

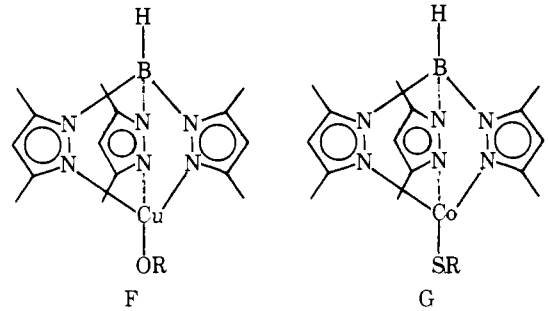

F G

$CoN_3(SR)$ compounds of structure G,[29] our results provide useful insight into some of the most distinctive and structure/function-sensitive features of the type 1 core.

Experimental Section

All chemicals were reagent grade and were used as received, unless otherwise noted. The solvents tetrahydrofuran (THF), hexane, and

diethyl ether were distilled from sodium–potassium alloy benzophenone ketyl under prepurified nitrogen. All other solvents were stored over molecular sieves (4A) and were deaerated with prepurified nitrogen prior to use. Standard Schlenk ware, glovebag, and glovebox techniques were used in the handling of air-sensitive complexes. Elemental analyses were performed by Micro-Tech Laboratories, Inc., Skokie, Ill., and by H. Beck, Analytical Services Laboratory, Chemistry Department, Northwestern University, Evanston, Ill.

Preparation of Potassium Hydrotris(3,5-dimethyl-1-pyrazolyl)borate, $KHB(3,5\text{-}Me_2pz)_3$. The literature procedure was used in the preparation of this compound.[30] Three sublimations at 280 °C under high vacuum were necessary to obtain a white solid with a melting point of 295–298 °C. The potassium salt has a B–H stretching frequency at 2445 cm^{-1}.

Preparation of Potassium *p*-Nitrobenzenethiolate, $K[SC_6H_4NO_2]$. Technical grade (85+ %) *p*-nitrobenzenethiol was purified according to the literature procedure[31] with a slight modification. Under nitrogen the mercaptan (2.5 g, 0.016 mol) was heated in 30 mL of absolute ethanol with KOH (0.90 g, 0.016 mol) to produce an intensely red solution. The solution was next filtered under nitrogen at the boiling point to remove the yellow, insoluble disulfide, $(SC_6H_4NO_2)_2$. The red filtrate can be stored under nitrogen and used for subsequent syntheses requiring *p*-nitrobenzenethiolate.

Preparation of *p*-Nitrobenzenethiolatocopper(II) Perchlorate Hemiethanolate, $[Cu(SC_6H_4NO_2)](ClO_4)\cdot{}^1/_2(CH_3CH_2OH)$. The red, ethanolic solution of $KSC_6H_4NO_2$, prepared in the manner described above, was added dropwise in approximately 0.5 h under nitrogen to a vigorously stirred solution of $Cu(ClO_4)_2\cdot 6H_2O$ (5.4 g, 0.015 mmol) in 25 mL of ethanol. The solvent was removed under high vacuum to yield an orange solid, which was washed with distilled water and dried under vacuum. Anal. Calcd for $C_7H_7ClCuNO_{6.5}S$: C, 24.71; H, 2.07; N, 4.12. Found: C, 25.70; H, 1.91; N, 4.40. Infrared data in cm^{-1} (Nujol mull): 3410 w, br, 1560 s, 1330 s, 1095 s, 1075 s, 835 m, 745 s.

Preparation of *O*-Ethylcysteinatocopper(II) Perchlorate, $[Cu(SCH_2CH(NH_2)(COOC_2H_5)](ClO_4)$. To *O*-ethylcysteinate monohydrate monochloride (1.6 g, 8.6 mmol) in approximately 10 mL of ethanol was added potassium hydroxide (1.1 g, 0.017 mol). This solution was added slowly to a stirred solution of $Cu(ClO_4)_2\cdot 6H_2O$ (3.4 g, 9.2 mmol) in approximately 10 mL of ethanol. Removal of the solvent under high vacuum yielded a dark blue solid, which was washed with water and dried under high vacuum. Infrared data in cm^{-1} (Nujol mull): 3200 w, br, 1730 m, 1600 w, br, 1140 m, 1090 s, 630 m.

Preparation of Potassium *p*-Nitrobenzenethiolato(hydrotris(3,5-dimethyl-1-pyrazolyl)borato)cuprate(I) Diacetone, $K[Cu(HB(3,5\text{-}Me_2pz)_3)(SC_6H_4NO_2)]\cdot 2C_3H_6O$ (1a). An ethanolic solution (40 mL) of potassium *p*-nitrobenzenethiolate (1.2 g, 6.2 mmol) was prepared as described above. This solution was added dropwise in approximately 0.5 h under nitrogen to a vigorously stirred solution of CuCl (0.61 g, 6.2 mmol, Rocky Mountain Research, 99.999%) in 10 mL of ethanol. After the solution was stirred for 0.5 h, the solvent was removed under high vacuum to yield a reddish-brown solid. This solid was next added at room temperature to a stirred acetone solution (20 mL) of $KHB(3,5\text{-}Me_2pz)_3$ (2.1 g, 6.2 mmol) to yield a purple solution, which was stirred for approximately 0.5 h. Filtration and evaporation of solvent yielded a dark brown solid. Anal. Calcd for $C_{27}H_{38}BCuKN_7O_4S$: C, 48.39; H, 5.72; N, 14.63. Found: C, 47.20; H, 5.13; N, 13.77. Infrared data in cm^{-1} (Nujol mull): 2505 w, 1575 s, 1500 w, 1300 s, 1185 s, 1105 w, 1085 s, 1065 m, 845 w, 815 w, 795 w, 775 w, 735 w.

The complex **1a** can also be synthesized by another route. To a vigorously stirred acetone solution (20 mL) of $KHB(3,5\text{-}Me_2pz)_3$ (2.1 g, 6.2 mmol) was added $[Cu(SC_6H_4NO_2)]ClO_4\cdot{}^1/_2CH_3CH_2OH$ (2.0 g, 6.2 mmol). The solution turned intensely blue and, immediately thereafter, purple. Filtration of the solution and slow evaporation of the solvent gave a dark reddish-brown powder, **1a**, and light blue crystals of $Cu(HB(3,5\text{-}Me_2pz)_3)_2$.[30a] These complexes were separated by the addition of acetone followed immediately by filtration to remove the light blue Cu^{II} complex. Removal of the solvent under high vacuum or the addition of ether–hexane to the resulting solution gave **1a**.

Preparation of Potassium *O*-Ethylcysteinato(hydrotris(3,5-dimethyl-1-pyrazolyl)borato)cuprate(I), $K[Cu(HB(3,5\text{-}Me_2pz)_3)(SCH_2CH(NH_2)(COOC_2H_5)]\cdot C_3H_6O$ (1b). L-*O*-Ethylcysteine monohydrate hydrochloride (1.6 g, 8.6 mmol) was dissolved in ethanol and mixed with KOH (1.1 g, 0.017 mol) under an inert atmosphere. This solution was added dropwise in 0.5 h to a stirred ethanol solution (20 mL) of CuCl (0.85 g, 8.6 mmol) to give a colorless solution. The solvent was removed under high vacuum to yield a white solid. This solid was added to a stirred acetone solution of $KHB(3,5\text{-}Me_2pz)_3$ (2.9 g, 8.6 mmol). Removal of the solvent under high vacuum gave a colorless solid. Anal. Calcd for $C_{23}H_{38}BCuKN_7O_3S$: C, 45.58; H, 6.32; N, 16.18. Found: C, 45.49; H, 6.62; N, 15.04. Infrared data in cm^{-1} (Nujol mull): 3300 w, 2510 w, 1700 s, 1540 s, 1250 s, 1200 s, 1070 s, 1030 m, 980 w, 830 m, 805 s, 790 m, 770 s, 730 w, 700 w, 655 m.

Preparation of *p*-Nitrobenzenethiolato(hydrotris(3,5-dimethyl-1-pyrazolyl)borato)copper(II), $Cu(HB(3,5\text{-}Me_2pz)_3)(SC_6H_4NO_2)$ (2a). The orange solid $[Cu(SC_6H_4NO_2)](ClO_4)\cdot{}^1/_2CH_3CH_2OH$ (0.1 g, 0.3 mmol) described above was added to a stirred THF (10 mL) solution of $KHB(3,5\text{-}Me_2pz)_3$ (0.1 g, 0.33 mmol) at −78 °C to yield an intensely blue solution. After 5 h of stirring, the solution was filtered at −78 °C, and the solvent removed under high vacuum at −30 °C (bromobenzene slush) to yield a dark blue-black powder. Anal. Calcd for $C_{21}H_{26}BCuN_7O_2S$: C, 49.0; H, 5.06; N, 19.0. Found: C, 47.2; H, 6.00; N, 18.71. Infrared data in cm^{-1} (Nujol mull): 2500 w, 1560 s, 1300 s, 1180 s, 1070 s, 1020 m, 850 m, 835 m, 800 m, 770 m, 720 m.

Preparation of *O*-Ethylcysteinato(hydrotris(3,5-dimethyl-1-pyrazolyl)borato)copper(II), $Cu(HB(3,5\text{-}Me_2pz)_3)(SCH_2CH(NH_2)(COOC_2H_5))$ (2b). The blue solid $[Cu(SCH_2CH(NH_2)(COOC_2H_5))](ClO_4)$ (0.8 g, 3.8 mmol) described above was added to a stirred THF solution (10 mL) of $KHB(3,5\text{-}Me_2pz)_3$ (0.80 g, 2.4 mmol) at −78 °C to yield an intensely blue solution. Filtration and removal of the solvent at −37 °C (anisole slush) yielded a blue-black solid, which lost its dark color on warming to room temperature.

Preparation of *p*-Nitrophenolato(hydrotris(3,5-dimethyl-1-pyrazolyl)borato)copper(II), $Cu(HB(3,5\text{-}Me_2pz)_3)(OC_6H_4NO_2)$ (3). To a stirred 20-mL THF solution of $CuBr_2$ (0.24 g, 1.1 mmol) at room temperature was added $KHB(3,5\text{-}Me_2pz)_3$ (0.37 g, 1.1 mmol). After the solution was stirred for approximately 0.5 h, sodium *p*-nitrophenolate dihydrate (0.22 g, 1.1 mmol) was added slowly. An emerald-green solution developed within 0.5 h. The solution was filtered, and the solvent removed under high vacuum to yield a green powder. Anal. Calcd for $C_{21}H_{26}BCuN_7O_3$: C, 50.56; H, 5.25; N, 19.66. Found: C, 50.68; H, 5.80; N, 18.37. Infrared data in cm^{-1} (Nujol mull): 2505 w, 1669 w, 1590 s, 1540 s, 1300 s, 1260 m, 1200 s, 1105 s, 1080 s, 1020 s, 850 m, 805 s, 770 m.

Spectral Studies. Infrared spectra were obtained on Nujol mulls with a Perkin-Elmer 337 or 727B infrared spectrophotometer. Mulls were prepared in a glovebag under prepurified nitrogen. UV–visible and near-infrared spectra were obtained with a Cary 17D spectrometer. Complexes **2a** and **2b** were studied under nitrogen in a low-temperature cell at −78 °C. All other complexes were studied in 1-cm cells fitted with Schlenk connections. EPR spectra were obtained on a Varian E-4 X-band spectrometer and were calibrated with diphenylpicrylhydrazyl (g = 2.0036) or Varian strong pitch (g = 2.0028).[32] THF glasses or solid samples were used at −196 °C in quartz capillary tubes fitted with Schlenk connections. Laser Raman spectra were observed with Ar^+ (5145 Å) or Kr^+ (6471 Å) excitation sources. A Spex 1401 monochromator and photon counting detection were used. Samples of **1a, 1b,** and **3** were examined as powders. Spectra of **2a** were recorded in THF solutions at −80 °C. All samples were spun at 1800 rpm in 12-mm Pyrex tubes under nitrogen.

X-ray Data Collection for $K[Cu(HB(3,5\text{-}Me_2pz)_3)(SC_6H_4NO_2)]\cdot 2C_3H_6O$. Dark brown crystals, marginally suitable for X-ray diffraction study, were prepared via the second synthetic procedure described above and were grown from an acetone–hexane–ether solution at −10 °C. A representative crystal was mounted in a glass capillary in a glovebox under an inert atmosphere. An examination of the crystal by Weissenberg and precession methods established that it belongs to the triclinic system. The assumption of space group C_i^1-$P\bar{1}$ was confirmed ultimately by the successful refinement of the structure. The six faces of the crystal were identified as belonging to {010}, {210}, {01$\bar{4}$}. The lattice constants were determined by a least-squares analysis[33] of the angle settings of 16 hand-centered reflections on a Picker FACS-1 diffractometer in the range $20° > 2\theta > 11°$ (Mo $K\alpha_1$ radiation, λ = 0.709 30 Å). The refined cell constants and other relevant crystal data are given in Table I. Owing to the tendency of the material to lose solvent, an observed density was not obtained.

Intensity data were collected by the ω scan technique with graphite-monochromatized Mo $K\alpha$ radiation at a takeoff angle of 4.2°. The counter preceded by an aperture 5.3 mm high and 4.6 mm wide was positioned 32 cm from the crystal. Each peak was scanned through 8° in ω with 81 one-second steps. Stationary-crystal, stationary-

Table I. Crystal Data for K[Cu(HB(3,5-Me$_2$pz)$_3$)(SC$_6$H$_4$NO$_2$)]·2C$_3$H$_6$O

molecular formula	$C_{27}H_{38}BCuKN_7O_4S$
mol wt	670.17 amu
a	10.60 (2) Å
b	18.17 (4) Å
c	10.33 (4) Å
α	93.57 (5) Å
β	116.20 (7)°
γ	71.89 (5)°
V	1690 Å^3
Z	2
space group	C_i^1-$P\bar{1}$
crystal dimensions	0.29 × 0.15 × 0.07 mm
radiation	Mo Kα_1 (λ = 0.709 300 Å), monochromatized from mosaic graphite
scan speed	0.1°/s in ω
scan range	8° in ω
receiving aperture	5.3 × 4.6 mm, 32 cm from crystal
background counting time	20 s
2θ limits	2.5–31°
temp	25 °C
absorption coefficient	8.7 cm^{-1}
transmission factors	0.89–0.94
unique data used ($F_o^2 > 3\sigma(F_o^2)$)	678
number of variables	117
R	0.092
R_w	0.097

Table II. Positional and Thermal Parameters for the Nongroup Atoms of K[Cu(HB(3,5-Me$_2$pz)$_3$)(SC$_6$H$_4$NO$_2$)]·2C$_3$H$_6$O

ATOM	X[A]	Y	Z	B11 OR B,A^2
CU	-0.19471(74)	-0.26550(32)	0.27248(68)	207.(12)
S	-0.4211(14)	-0.21442(69)	0.1030(14)	7.64(42)
K	-0.0532(12)	-0.19866(61)	-0.3478(12)	9.06(38)
B	0.1566(57)	-0.3631(29)	0.4952(58)	6.7(16)
O(41)	-0.0557(35)	-0.0519(17)	-0.2061(35)	9.07(94)
O(42)	-0.2317(36)	-0.0326(18)	-0.4336(40)	11.3(12)
O(1)	-0.3012(32)	-0.1559(17)	-0.2867(36)	9.45(96)
O(2)	0.1588(52)	-0.2634(26)	-0.0782(53)	17.7(18)
N(48)	-0.1891(50)	-0.0168(24)	-0.3076(53)	9.3(13)
C(1)	-0.1769(55)	-0.1552(26)	-0.0397(55)	9.0(15)
C(2)	-0.3165(67)	-0.1323(30)	-0.1662(64)	10.2(16)
C(3)	-0.4797(58)	-0.0827(28)	-0.2122(52)	10.4(16)
C(4)	0.3827(60)	-0.3579(30)	0.0491(55)	11.6(18)
C(5)	0.2456(79)	-0.2943(40)	0.0351(79)	13.2(22)
C(6)	0.2325(49)	-0.2589(26)	0.1712(56)	10.2(16)

B22	B33	B12	B13	B23
19.4(26)	162.(13)	3.0(40)	107.(10)	-7.9(40)

[a] Estimated standard deviations in the least significant figure(s) are given in parentheses in this and all subsequent tables. [b] The form of the anisotropic thermal ellipsoid is: $\exp(-(B11h^2 + B22k^2 + B33l^2 + 2B12hk + 2B13hl + 2B23kl))$. The quantities given in the table are the thermal coefficients ×10^4. The $B22$, $B33$, $B12$, $B13$, and $B23$ values are for Cu.

counter background counts of 20 s were taken at the beginning and end of each scan.[34] Attenuation of the peaks was not necessary. Intensity data for $\pm h$, $\pm k$, and $+l$ were collected out to $2\theta = 31°$. Because of the poor crystal quality, only a limited data set could be collected. During the data collection, six standard reflections were collected after every 100 reflections. There was no significant variation of their intensities during the data collection.

The intensity data were processed as previously described[33] with the parameter p chosen as 0.04. Of the 1528 unique reflections collected, 678 had $F_o^2 > 3\sigma(F_o^2)$ and were used in the subsequent solution and refinement of the structure.

Solution and Refinement of the Structure. Based on direct methods, the Cu, S, and Cu-bonded N atoms were found in an E map. A series of full-matrix least-squares refinements and concomitant difference maps were required to find all nonhydrogen atoms. Each of the four rings in the molecule was refined as a rigid group.[35] Bond angles and bond distances for a 3,5-dimethylpyrazole group[28] and for a p-nitrobenzenethiolate group[31] from previously reported crystal structure studies were used to define the rigid groups. Atomic scattering factors were taken from Cromer's and Waber's tabulation.[36] With isotropic temperature factors for all nonhydrogen atoms, the structure refined to $R = 0.144$ and $R_w = 0.151$, where $R = \Sigma||F_c| - |F_o||/\Sigma|F_o|$ and $R_w = (\Sigma w(|F_o| - |F_c|)^2/\Sigma(wF_o^2))^{1/2}$.

Before proceeding further with the refinement, an absorption correction was applied to the data. The transmission coefficients ranged from 0.888 to 0.941 (μ = 8.68 cm^{-1}). A final least-squares cycle in which the Cu atom was refined anisotropically was carried out. This cycle with 678 independent reflections and 117 variables refined to values of R and R_w of 0.092 and 0.097. The largest peaks in the final difference Fourier map were approximately 0.4 e/Å^3 in height.

The final positional and thermal parameters for the nongroup atoms, along with their estimated standard deviations, are given in Table II. Table III lists the derived parameters for the atoms belonging to the four rigid groups. Table IV lists $10|F_o|$ vs. $10|F_c|$.[37] The root mean square amplitudes of vibration for the Cu atom are 0.154 (12), 0.250 (11), and 0.319 (8) Å.

Results and Discussion

Synthetic Approach. To synthesize complexes of the general stoichiometry CuN$_3$(SR) and of stereochemistry A, several facets of copper chemistry must be recognized. Although approximately tetrahedral coordination geometries and the binding of mercaptide ligands are not implausible for Cu^I, their appearance is contrary to the great bulk of experience in Cu^{II} chemistry.[38] By far the most stable coordination geometry for Cu^{II} is square planar or tetragonally distorted (4 + 1 or 4 + 2) octahedral.[2,38] Only very bulky or stereochemically specific (and rigid) ligands can force four-coordinate cupric structures away from square-planar toward tetrahedral coordination polyhedra when the ligands are neutrally charged.[2,38] Indeed, stable low molecular weight cationic tetrahedral complexes of the first-row transition metals are rare, especially those of the Cu^{II} ion.[38-40] However, neutral and anionic tetrahedral Cu^{II} complexes are more common. Therefore, in the synthesis of pseudotetrahedral copper(II)-mercaptide complexes, we chose an N$_3$ donor ligand with a negative charge. In the present synthetic investigation, the mononegative hydrotris(3,5-dimethyl-1-pyrazolyl)borate ligand, D, was chosen for the N$_3$ portion of the coordination sphere. In prior work[28] we have studied the chemistry and structures of Cu^I complexes of ligands C and D. These ligands are known to constrain copper and other metal ions to nonplanar, trigonal MN$_3$ interactions. Furthermore, cupric ions generally oxidize mercaptides to disulfides:[38b,41]

$$2Cu^{2+} + 2SR^- \rightleftharpoons 2Cu^+ + RSSR \quad (1)$$

The trispyrazolylborate ligands have been shown to donate appreciable electron density to copper ions, as judged by the relatively low energies of the CO stretching frequencies in Cu(HB(R$_2$pz)$_3$)(CO) compounds.[42] We anticipated that the use of this particular ligand would inhibit reduction of the cupric ion. The methylated pyrazolylborate ligand (D) was chosen because it is a stronger electron donor than C[42] and because we anticipated that the methyl substituents would maximize solubility and minimize molecular aggregation. The possibility of stabilizing Cu^{II} by appropriate choice of mercaptide ligand we also recognized, and the first experiments were conducted with the less readily oxidized mercaptide, p-nitrobenzenethiolate.[31]

The preparation of the monovalent CuN$_3$(SR) derivatives is straightforward and is presented in eq 2 and 3. The presumably polymeric cuprous mercaptides, Cu^I(SR), were used as reagents and were not characterized in detail. The

Table III. Derived Parameters for the Rigid Group Atoms of $K[Cu(HB(3,5\text{-}Me_2pz)_3)(SC_6H_4NO_2)]\cdot 2C_3H_6O$

ATOM	X	Y	Z	B, Å^2	ATOM	X	Y	Z	B, Å^2
C(41)	0.4719(35)	-0.1444(12)	0.1705(41)	5.5(12)	N(22)	0.0343(25)	-0.3690(12)	-0.4786(22)	6.51(96)
C(42)	0.3275(41)	-0.1091(18)	0.0680(22)	5.3(12)	C(21)	-0.1721(21)	-0.3613(10)	-0.4566(19)	6.0(12)
C(43)	0.2279(22)	-0.0559(16)	0.1081(34)	5.9(12)	C(22)	-0.0605(23)	-0.4212(11)	-0.3571(21)	7.2(13)
C(44)	0.2728(35)	-0.0380(13)	0.2507(42)	7.9(14)	C(23)	0.0653(21)	-0.42633(97)	-0.3696(19)	5.2(11)
C(45)	0.4173(41)	-0.0734(18)	0.3533(22)	5.2(11)	C(24)	-0.3313(22)	-0.3303(16)	-0.4898(32)	8.1(14)
C(46)	0.5168(22)	-0.1266(16)	0.3132(33)	5.1(11)	C(25)	0.2122(23)	-0.4845(14)	-0.2799(28)	6.9(12)
N(11)	-0.0604(22)	-0.3492(10)	0.2143(24)	6.39(98)	N(31)	-0.0236(22)	-0.2163(12)	-0.6229(21)	6.17(93)
N(12)	0.0821(24)	-0.3769(11)	0.3217(19)	7.8(11)	N(32)	0.1076(26)	-0.27059(98)	-0.5341(23)	6.49(98)
C(11)	-0.0598(20)	-0.38158(89)	0.0836(20)	5.3(12)	C(31)	0.0019(21)	-0.1420(10)	-0.6048(19)	7.4(13)
C(12)	0.0813(21)	-0.4285(10)	0.1110(19)	5.2(12)	C(32)	0.1468(23)	-0.1511(11)	-0.5062(22)	5.8(12)
C(13)	0.1682(20)	-0.42603(86)	0.2554(19)	6.7(13)	C(33)	0.2118(21)	-0.2290(12)	-0.4626(19)	8.7(15)
C(14)	-0.1982(23)	-0.3629(15)	-0.0544(24)	6.8(13)	C(34)	-0.1192(27)	-0.0702(13)	-0.6866(28)	7.2(13)
C(15)	0.3301(20)	-0.4695(13)	0.3291(27)	4.1(11)	C(35)	0.3701(22)	-0.2633(17)	-0.3552(28)	10.6(16)
N(21)	-0.1140(25)	-0.3284(10)	-0.5329(20)	6.34(94)					

RIGID GROUP PARAMETERS

GROUP	x_C, Å	y_C, Å	z_C, Å	DELTA, rad	EPSILON, rad	ETA, rad
RING1	0.3724(19)	-0.09122(88)	0.2106(20)	1.657(25)	2.367(23)	1.052(22)
RING2	0.0461(19)	-0.39576(70)	0.1895(18)	0.639(25)	-2.074(12)	0.786(24)
RING3	-0.0502(21)	-0.38497(82)	-0.4314(15)	-0.125(15)	2.314(15)	-0.113(14)
RING4	0.0944(20)	-0.19726(97)	-0.5423(16)	2.695(11)	-3.267(14)	2.8984(94)

[a] X_C, Y_C, and Z_C are the fractional coordinates of the origin of the rigid group. [b] The rigid group orientation angles δ, ϵ, and η (rad) have been defined previously: S. J. La Placa and J. A. Ibers, *Acta Crystallogr.*, **1965,** *18,* 511–519.

$$CuCl + K(SR) \xrightarrow{\text{ethanol}} Cu(SR) + KCl \quad (2)$$

$$Cu(SR) + KHB(3,5\text{-}Me_2pz)_3 \xrightarrow[\text{room temperature}]{\text{acetone}} K[Cu(HB(3,5\text{-}Me_2pz_3)(SR)] \quad (3)$$

1a, SR = *p*-$SC_6H_4NO_2$

b, SR = *O*-ethylcysteinate

$Cu^IN_3(SR)$ complexes were characterized by elemental analysis as well as by infrared and laser Raman spectroscopy. The *O*-ethylcysteinate complex is colorless as are the reduced forms of the type 1 sites, but the *p*-nitrobenzenethiolate derivative has a violet color (λ 550 nm, ϵ 9600 M^{-1} cm^{-1}), which arises within the mercaptide functionality (vide infra). The energy and intensity of this intraligand optical transition are dependent on the oxidation state of the coordinated metal ion. Single crystals of **1a** marginally suitable for X-ray diffraction studies can be grown from acetone–ether–hexane mixtures at −10 °C. The molecular structure of this complex, which corresponds to configuration E, is discussed in a following section.

The synthetic approach to the $Cu^{II}N_3(SR)$ complexes is shown in eq 4[43] and 5. It can also be applied to other mercaptides (e.g., $^-SC_6F_5$).[44] The intermediate $[Cu(SR)](ClO_4)$ reagents are insoluble in all common solvents and appear to be oligomeric. These complexes were not characterized in detail. That the powder EPR spectrum at liquid nitrogen temperature consists of a broad, structureless band is consistent with a polymer incorporating Cu^{II} ions. The reaction of the $[Cu(SR)](ClO_4)$ reagents with $KHB(3,5\text{-}Me_2pz)_3$ at low temperatures (eq 5) produces deep blue solutions of the Cu^{II} mercaptide complexes **2a** and **2b**. Great caution must be exercised in handling these solutions because thermal decomposition is rapid, especially for **2b,** above ca. −30 °C. Low-temperature filtration of the reaction mixtures and vacuum evaporation of the solvent at ca. −30 °C yield blue-black solids. These fade in color on warming to room temperature under nitrogen; elemental analysis and the infrared spectrum of the warmed solid are consistent with the $Cu(HB(3,5\text{-}Me_2pz)_3)(SC_6H_4NO_2)$ stoichiometry for **2a.** As will be discussed in following sections, all spectral data on the products maintained at low temperature are consistent with the monomeric, cupric structure E (i.e., A where X = N) and also with the stoichiometry of eq 5 as written.[44]

$$Cu(ClO_4)_2 + KSR \xrightarrow{\text{ethanol}} [Cu(SR)](ClO_4) + KClO_4 \quad (4)$$

$$[Cu(SR)](ClO_4) + KHB(3,5\text{-}Me_2pz)_3 \xrightarrow[-78\ ^\circ C]{THF} Cu(HB(3,5\text{-}Me_2pz)_3)(SR) + KClO_4 \quad (5)$$

2a, SR = *p*-$SC_6H_4NO_2$

b, SR = *O*-ethylcysteinate

Additional support for the proposed constitution of **2a** and **2b** is derived from chemical experiments. Redox connection between **1a** and **2a** is demonstrated by the quantitative reduction of **2a** using potassium metal at −78 °C to produce **1a:**

$$Cu(HB(3,5\text{-}Me_2pz)_3)(SC_6H_4NO_2) \xrightarrow[-78\ ^\circ C,\ THF]{K} [Cu(HB(3,5\text{-}Me_2pz)_3)(SC_6H_4NO_2)]^- \quad (6)$$

In addition, it is possible to synthesize the phenolate analogue of **2a** using the approach

$$CuBr_2 + KHB(3,5\text{-}Me_2pz)_3 \xrightarrow{THF} CuBr(HB(3,5\text{-}Me_2pz)_3) + KBr \quad (7)$$

$$CuBr(HB(3,5\text{-}Me_2pz)_3) + Na(p\text{-}OC_6H_4NO_2) \xrightarrow{THF} Cu(HB(3,5\text{-}Me_2pz)_3)(OC_6H_4NO_2)\ (\mathbf{3}) + NaBR \quad (8)$$

As expected from the poor reducing ability of phenolate vis-à-vis thiophenolate, **3** is indefinitely stable at room temperature. In work to be discussed in detail elsewhere, a dithiocarbamate analogue of **2** has also been synthesized:[44b]

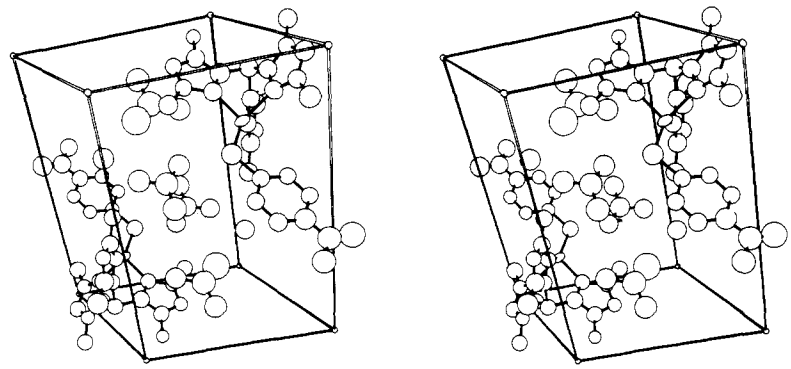

Figure 1. Stereoview of the unit cell of $K[Cu(HB(3,5\text{-}Me_2pz)_3)(SC_6H_4NO_2)]\cdot 2C_3H_6O$. The y axis is almost vertical, and the x axis is horizontal and to the right. Vibrational ellipsoids are drawn at the 30% probability level.

$$Cu(S_2CN(CH_3)_2)Cl + KHB(3,5\text{-}Me_2pz)_3 \xrightarrow{THF} Cu(HB(3,5\text{-}Me_2pz)_3)(S_2CN(CH_3)_2) + KCl \quad (9)$$

The dithiocarbamate ligand is known to be compatible with relatively high metal oxidation states, and, in accord with this, the dark green complex **4** is stable at room temperature. It has been characterized by elemental analysis, molecular weight in benzene, and EPR spectroscopy.[44b] Finally, further support for the formulation of **2** is derived from the synthesis of thermally stable cobalt(II) analogues, **5** (eq 10 and 11), which have been characterized by a variety of chemical and physical methods including, for **5c**, single-crystal X-ray diffraction. These compounds are discussed in an accompanying article.[29]

$$CoBr_2 + KHB(3,5\text{-}Me_2pz)_3 \xrightarrow{THF} CoBr(HB(3,5\text{-}Me_2pz)_3) + KBr \quad (10)$$

$$CoBr(HB(3,5\text{-}Me_2pz)_3) + NaSR \xrightarrow{THF} Co(HB(3,5\text{-}Me_2pz)_3)(SR) + NaBr \quad (11)$$

5a, SR = *O*-ethylcysteinate
b, SR = *p*-$SC_6H_4NO_2$
c, SR = SC_6F_5

The course of reaction 5 was, in addition, investigated for the *p*-nitrobenzenethiolate system at room temperature. Upon combining the reactants an intense blue solution is obtained which, in the course of several seconds, turns deep violet. The products that can be isolated from this reaction mixture (see Experimental Section for details) include the disulfide, $(SC_6H_4NO_2)_2$, the cuprous pyrazolylborate mercaptide, **1a**, and the known bis(hydrotris(3,5-dimethylpyrazolyl)borate) complex, $Cu(HB(3,5\text{-}Me_2pz)_3)_2$. Although the use of a strongly electron-withdrawing mercaptan did not allow the synthesis of $Cu^{II}N_3(SR)$ complexes that are stable at room temperature, greater thermal stability is achieved with SR = *p*-$SC_6H_4NO_2$ than with SR = *O*-ethylcysteinate. This trend can be extended to other mercaptides; the complex with SR = SC_6F_5 is stable at ca. −10 °C.[44]

Interestingly, solutions of **2a** and **2b** yield green $Cu^{II}SO_2R$ complexes when they are warmed to room temperature in the presence of oxygen. The XPS spectra of these green complexes in the sulfur 2p region indicate the presence of oxidized sulfur.[20,45] The EPR spectra of the oxygenated complexes prepared from both **2a** and **2b** resemble those of the parent compound and are therefore diagnostic of a pseudotetrahedral copper(II)-$HB(Me_2pz)_3$ complex (vide infra). There are bands in the infrared spectrum of each of these complexes in the 1250–1000-cm^{-1} region that are absent from the spectrum of the parent complex and that are suggestive of an $M\text{-}SO_2R$ complex.[46] There are other examples in the literature of the synthesis of sulfinato complexes by the oxidation of mercaptides or disulfides.[47] These reactions may be models for the oxidation of cysteine in biological systems, which is an important reaction in the production of sulfates. Although the reaction mechanism is not well understood, cysteine is oxidized to cysteine sulfinate in the presence of cysteine dioxygenase, oxygen, Fe(II) ions, and NADH or NADPH.[48]

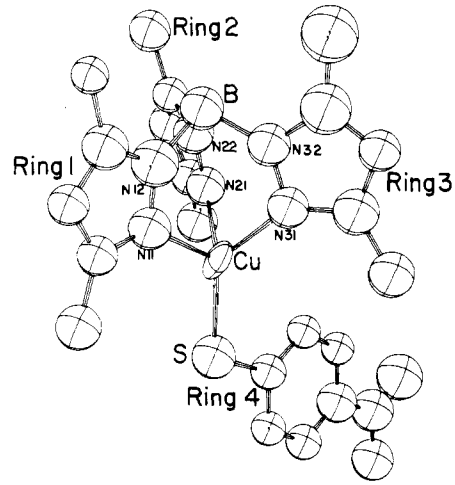

Figure 2. The molecular structure of the anionic portion of $K[Cu(HB(3,5\text{-}Me_2pz)_3)(SC_6H_4NO_2)]\cdot 2C_3H_6O$ (the 50% probability thermal ellipsoids are shown).

Description of the Structure of $K[Cu(HB(3,5\text{-}Me_2pz)_3)(SC_6H_4NO_2)]\cdot 2C_3H_6O$ (1a). The overall structure of the $K[Cu(HB(3,5\text{-}Me_2pz)_3)(SC_6H_4NO_2)]\cdot 2C_3H_6O$ complex is apparent in the stereoscopic drawing of the unit cell (Figure 1). The structure consists of monomeric $[Cu(HB(3,5\text{-}Me_2pz)_3)(SC_6H_4NO_2)]^-$ anions (Figure 2), K^+ cations, and acetone of solvation. The CuN_3S coordination sphere may be described as highly distorted tetrahedral. The ligand $HB(3,5\text{-}Me_2pz)_3^-$ coordinates to the Cu ion through the N atom in the 2 position of each of the pyrazole rings and bonds in a manner typical of other monomeric pyrazolylborate compounds.[29,42] In Figure 2 note that the methyl groups in the 3 position do provide some steric protection for the Cu ion. The *p*-nitrobenzenethiolate ligand is coordinated to the Cu atom through the S atom.

The considerable distortion of the copper coordination geometry from T_d symmetry can be seen more clearly in Figure 3. The N-Cu-S bond angles are all in excess of 109.5°, and the N-Cu-N angles are all less than this value. A similar elongation along the pseudo-threefold axis of the copper coordination polyhedron has been observed in the complexes

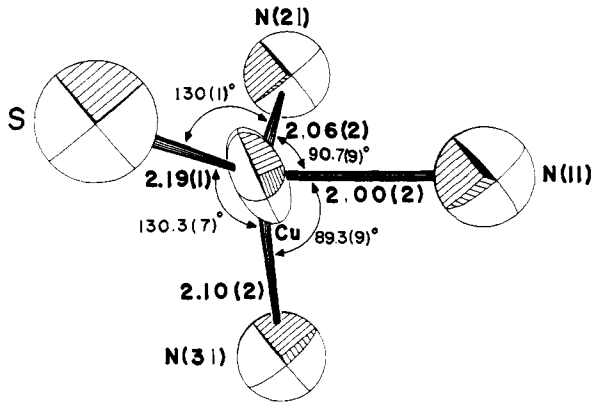

Figure 3. View of the coordination geometry about the copper atom in $K[Cu(HB(3,5\text{-}Me_2pz)_3)(SC_6H_4NO_2)]\cdot 2C_3H_6O$.

$Cu(HBpz_3)(CO)$[42] and $Co(HB(3,5\text{-}Me_2pz)_3)(SC_6F_5)$.[29] Such a distortion may be a consequence of the bonding restrictions imposed by the tris(pyrazolyl)borate ligand. It is important that the geometry of the copper coordination sphere in the present case is that of an elongated or trigonally distorted tetrahedron, and not that of a more irregularly distorted tetrahedron, which may be present in poplar plastocyanin.[23]

Selected bond distances and angles for **1a** are compiled in Table V.[49] Figure 4 shows the bond distances, bond angles, and numbering scheme used for the pyrazole rings. The Cu-N contacts are comparable with those in previously reported cuprous pyrazolylborate structures[29,42] and are in the range generally found for Cu^{I}-N bond distances.[2,50] Although the Cu-S distance of 2.19 (1) Å is somewhat shorter than the range of 2.199-2.429 Å observed in other structure determinations,[2,38h,51] we attribute no special significance to this short distance. One problem in comparing the Cu-S distance observed here with the literature values is that most of the latter are for S-bridging thiolate groups, thioethers, dialkyl sulfides, or thiourea.

The potassium ion is within 2.9 Å of two oxygen atoms of acetone molecules and the two oxygen atoms of a nitro group. In addition, atoms N(21) and N(31) are within 3.0 Å of the potassium ion. These values are typical of K-O and K-N distances.[52] Although the geometry about the K atom is distorted from octahedral symmetry, the coordination sphere is not unusual.[52] Judging from the literature, the K ion may also influence the coordination sphere of the Cu atom.[52] The N(21)-Cu-S and N(31)-Cu-S bond angles are approximately 130°, which is larger than the N-Cu-(CO) angles in $Cu(HBpz_3)(CO)$.[42] The influence of a positively charged counterion on an anionic metal coordination sphere has been observed in other structural studies.[52]

The geometry about the copper ion in these complexes is that of an elongated tetrahedron, largely imposed by the pyrazolylborate ligand. The idealized geometry of the N_3S copper coordination sphere is C_{3v}, with the threefold axis passing through the S, Cu, and B atoms. Figure 5 shows a view of the molecule along this idealized threefold axis. Although no crystallographic site symmetry is imposed on **1a**, it is evident from this figure that the geometry about the copper ion does not deviate appreciably from C_{3v}. The electronic and EPR spectra (vide infra) of **2a** and **2b** are consistent with near axial symmetry, but so are they in plastocyanin, which may be very distorted from C_{3v}.[23b] Based upon the aforementioned chemical data as well as the Raman and EPR data to be discussed in following sections, we propose that the structures of all of the $Cu^{I}(HB(3,5\text{-}Me_2pz)_3)(SR)^-$ and $Cu^{II}(HB(3,5\text{-}Me_2pz)_3)(SR)$ compounds reported here are similar, i.e., those illustrated in Figures 2 and 5.

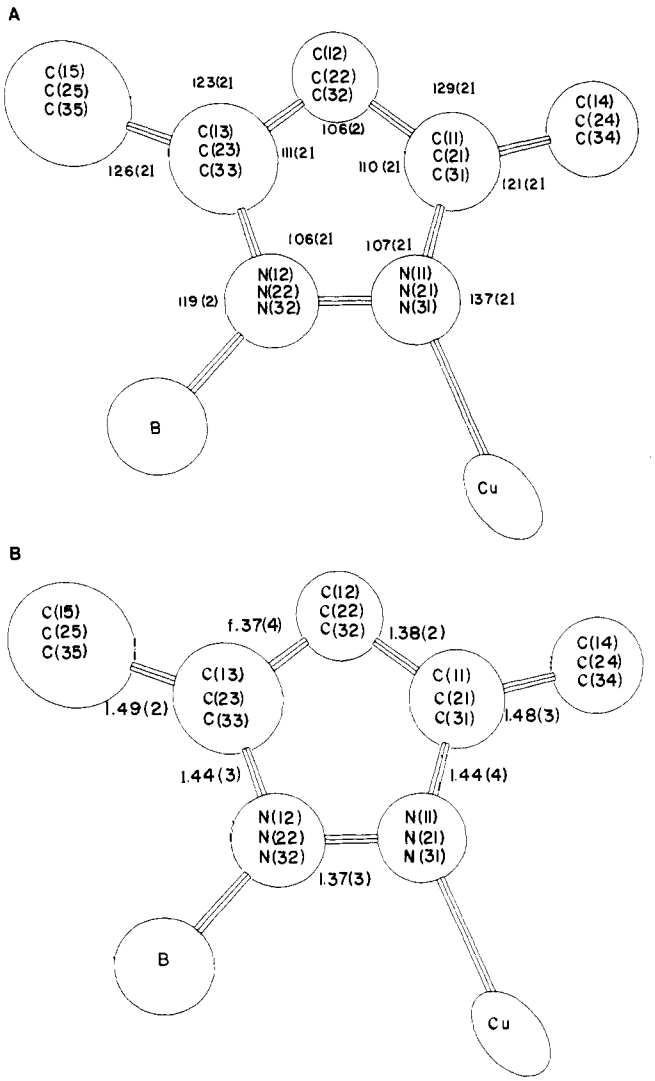

Figure 4. Bond angles (A), bond distances (B), and numbering scheme for the pyrazole rings.

Electronic Spectral Studies. Perhaps the most noticeable feature of compounds **2a** and **2b** is their intense blue color. Table VI compares optical data for the synthetic analogues with typical data for a number of blue copper proteins. There is a close similarity in band position and intensity: this similarity is illustrated in Figure 6 with data for *Pseudomonas aeruginosa* azurin.[1-6,18]

In viewing the $Cu^{II}(HB(3,5\text{-}Me_2pz)_3)(SR)$ data, it should be recognized that difficulties in handling such sensitive materials introduce inaccuracy in the molar absorption coefficients. The tabulated values were calculated on the basis of the quantities of reagents employed in the synthesis and assume both that the reaction has gone to completion and that no decomposition has occurred in transferring the solutions. If anything, we have underestimated the actual extinction coefficients.

As already noted, a distinctive feature of the oxidized type 1 site is the intense ($\epsilon \approx 3500$-6000 M^{-1} cm^{-1}) optical transition at 600 nm.[1-6,18] The proteins also usually exhibit weaker transitions at ca. 450 ($\epsilon \approx 300$-1000 M^{-1} cm^{-1}) and ca. 800 nm ($\epsilon \approx 400$ M^{-1} cm^{-1}); the intensities of these bands vary greatly from protein to protein.[1-6,18] Additional, very weak transitions have been observed in the near infrared.[19a,b] The origin of the 600-nm absorption has evoked considerable discussion, with the predominant conjecture being that it is sulfur

Table V. Selected Bond Distances (Å) and Angles (deg) for $K[Cu(HB(3,5\text{-}Me_2pz)_3)(SC_6H_4NO_2)]\cdot 2C_3H_6O$[a]

Cu-S	2.19 (1)	N(11)-Cu-N(21)	90.7 (9)
Cu-N(11)	2.00 (2)	N(11)-Cu-N(31)	89.3 (9)
Cu-N(21)	2.06 (2)	N(11)-Cu-S	115.7 (7)
Cu-N(31)	2.10 (2)	N(21)-Cu-N(31)	86.8 (9)
B-N(12)	1.65 (6)	N(21)-Cu-S	131.4 (10)
B-N(22)	1.47 (8)	N(31)-Cu-S	130.3 (7)
B-N(32)	1.60 (5)	N(12)-B-N(22)	96 (3)
S-C(41)	1.76 (4)	N(12)-B-N(32)	94 (3)
C(41)-C(42)	1.38 (4)	N(22)-B-N(32)	100 (3)
C(41)-C(46)	1.38 (5)	C(41)-S-Cu	110.8 (10)
C(42)-C(43)	1.39 (5)	C(42)-C(41)-S	114 (3)
C(43)-C(44)	1.38 (5)	C(46)-C(41)-S	126 (3)
C(44)-C(45)	1.38 (5)	C(42)-C(41)-C(46)	119 (3)
C(45)-C(46)	1.38 (4)	C(41)-C(42)-C(43)	120 (3)
C(44)-N(40)	1.40 (6)	C(42)-C(43)-C(44)	120 (2)
N(40)-O(41)	1.31 (4)	C(43)-C(44)-C(45)	120 (3)
N(40)-O(42)	1.22 (6)	C(44)-C(45)-C(46)	120 (3)
K-O(1)	2.84 (4)	C(45)-C(46)-C(41)	120 (3)
K-O(2)	2.72 (4)	N(40)-C(44)-C(43)	127 (3)
K-O(41)	2.96 (3)	N(40)-C(44)-C(45)	113 (3)
K-O(42)	2.96 (3)	O(1)-K-N(31)	133 (1)
K-N(31)	2.98 (3)	O(1)-K-N(32)	100 (1)
K-N(21)	2.99 (2)	O(2)-K-O(41)	83 (1)
C(2)-O(1)	1.35 (8)	O(2)-K-O(42)	127 (1)
C(2)-C(1)	1.43 (6)	O(2)-K-N(31)	127 (1)
C(2)-C(3)	1.55 (8)	O(2)-K-N(21)	108 (1)
C(5)-O(2)	1.16 (7)	O(41)-K-O(42)	44 (8)
C(5)-C(4)	1.56 (8)	O(42)-K-N(31)	121 (1)
C(5)-C(6)	1.55 (10)	O(41)-K-N(21)	168 (1)
		O(42)-K-N(31)	92 (1)
		O(42)-K-N(21)	124 (1)
		N(31)-K-N(21)	57 (1)
O(41)-N(40)-O(42)	123 (4)	O(1)-C(2)-C(1)	111 (5)
O(41)-N(40)-C(44)	111 (4)	O(1)-C(2)-C(3)	108 (4)
O(42)-N(40)-C(44)	126 (4)	C(1)-C(2)-C(3)	140 (6)
O(1)-K-O(2)	98 (2)	O(2)-C(5)-C(4)	119 (8)
O(1)-K-O(41)	73 (1)	O(2)-C(5)-C(6)	119 (6)
O(1)-K-O(42)	67 (1)	C(4)-C(5)-C(6)	121 (5)

[a] See text, Figure 3, and Figure 4 for numbering scheme.

(σS) → metal charge transfer in character.[6,9,18,53] The data for the $M(HB(3,5\text{-}Me_2pz)_3)(SR)$ compounds shed considerable light on this problem, and we are able to show conclusively by several lines of reasoning that this transition is indeed ligand-to-metal charge transfer in origin. Firstly, as has been noted before, the extinction coefficients of these bands are far too large to arise from Cu^{II} d-d transitions. Secondly, the displacement of the 600-nm absorption to higher energy as the mercaptide becomes more electron withdrawing (**2b** → **2a** → SR = SC_6F_5[44]) is exactly what is expected for ligand-to-metal charge transfer.[54] Thirdly, the energy of the 600-nm transition is predicted accurately by the empirical, optical electronegativity approach of Jørgensen.[55] As given in the equation

$$\nu_{CT}(cm^{-1}) = 30\,000(\chi_{ligand} - \chi_{metal}) \qquad (12)$$

the charge-transfer (CT) frequency is proportional to the difference in optical electronegativities of the ligand (χ_{ligand}) and the metal ion (χ_{metal}). The substitution of a tabulated[55] χ_{metal} for distorted tetrahedral Cu^{II} of 2.3 and a tabulated[55] χ_{ligand} of 2.9 (diethyl sulfide) or 2.8 (diethyl thiophosphate) yields a predicted ν_{CT} of 560–670 nm, which is in good agreement with the $CuN_3(SR)$ experimental data. Substituting the observed charge-transfer energies of **2a** or **2b** in eq 12 and χ_{metal} = 2.3,[55] we calculate χ_{ligand} values of 2.87 (*p*-nitrobenzenethiolate) and 2.79 (*O*-ethylcysteinate). These parameters along with a tabulated[55] χ_{metal} = 1.8 for tetrahedral Co^{II} predict ν_{CT} energies of 310–340 nm for the $Co(HB(3,5\text{-}Me_2pz)_3)(SR)$ complexes. As will be discussed in the accompanying contribution,[29] the experimental energies are 318 nm for SR = *p*-nitrobenzenethiolate and 340 nm for SR = *O*-ethylcysteinate.[29] Again, there is good agreement between theory and experiment when a charge-transfer transition is hypothesized. Finally, support for the spectral assignment in the $Cu(HB(3,5\text{-}Me_2pz)_3)(SR)$ compounds comes from observations on $Cu(HB(3,5\text{-}Me_2pz)_3)(OC_6H_4NO_2)$.

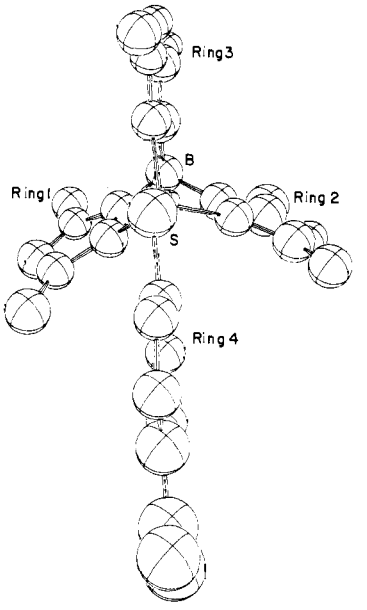

Figure 5. View of the $[Cu(HB(3,5\text{-}Me_2pz)_3)(SC_6H_4NO_2)]^-$ anion along S-Cu-B vector.

Table VI. Visible Absorption Data for $Cu(HB(3,5\text{-}Me_2pz)_3)(SC_6H_4NO_2)$ (**2a**), $Cu(HB(3,5\text{-}Me_2pz)_3)(SCH_2CH(NH_2)(COOC_2H_5))$ (**2b**), and Selected Blue Copper Proteins

	λ, nm	ε, M^{-1} cm^{-1}	ref
$Cu(HB(3,5\text{-}Me_2pz)_3)(SC_6H_4NO_2)$ (**2a**)	588	3900	
$Cu(HB(3,5\text{-}Me_2pz)_3)(SCH_2CH(NH_2)(COOC_2H_5))$ (**2b**)	680	2000	
Rhus vernicifera stellacyanin	605	4050	18d
			6
etiolated mung bean	598		6
Pseudomonas aeraginosa azurin	625	3500	6
	625	3500	18b
	625	5700	18c
spinach plastocyanin	597	4900	6
Polyporus versicolor laccase	610	4900	18d
Rhus vernicifera laccase	615	5700	18d

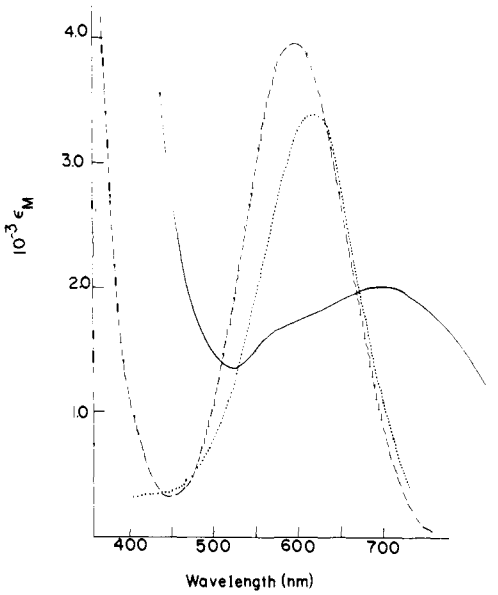

Figure 6. Optical spectra of **2a** (---) at −78 °C in THF, **2b** (—) at −78 °C in THF, and *Pseudomonas aeruginosa* azurin from ref 18b (·····).

Here an intense transition is not observed in the 600-nm region; rather only weak absorptions at 660 and 965 nm, typical of pseudotetrahedral Cu^{II} complexes,[56] are apparent. Use in eq 12 of $\chi_{ligand} = 3.2\text{-}3.3$ for oxygen-containing ligands yields a predicted $\nu_{CT} = 330\text{-}370$ nm for **3.** This result is consistent with the greater electronegativity of oxygen as compared with sulfur. The precise location of this transition in **3** is hindered owing to strong absorption in the same spectral region by the *p*-nitrophenolate and the tris(pyrazolyl)borate ligands.

Bands analogous to the weaker 450- and 800-nm transitions observed in most of the blue proteins are not evident in the absorption spectra of the $Cu(HB(3,5\text{-}Me_2pz)_3)(SR)$ derivatives.[57a] Since the synthetic analogues lack the bound methionine thioether sulfur atom present in some or all azurins and plastocyanins (and possibly in other blue proteins), it is possible that one or both of these bands in the proteins is associated with thioether ligand-to-metal charge transfer.[22,26,57b] Despite repeated attempts, $Cu(HB(3,5\text{-}Me_2pz)_3)(SR)$ transitions in the near-infrared region could not be located which were not unambiguously associated with solvent molecule vibrational overtones.

We attribute the intense purple color of **1a** (λ 550 nm, ε 9600 M^{-1} cm^{-1}) to an intraligand transition of the *p*-nitrobenzenethiolate functionality. The energy of this transition is highly sensitive to coordination of the sulfur atom. Ethanolic solutions of $K(SC_6H_4NO_2)$ are brilliant red in color (λ_{max} 420 nm), whereas the mercaptan, $HSC_6H_4NO_2$, is yellow in color (λ_{max} 317 nm). In **2a,** an intense band is observed at 380 nm, which is absent in **1a.** This shift of transition energy as the charge on the ligating atom is altered is typical of an intraligand transition.[54b]

Raman Studies. The blue copper proteins exhibit characteristic resonance-enhanced Raman vibrational scattering[58] when a laser excitation source is brought into coincidence with the 600-nm electronic transition.[12,26d] The oxidized forms of the proteins usually exhibit several transitions in the 350-450-cm^{-1} region and a single transition at approximately 270 cm^{-1}.[12] The former bands have been assigned to modes which are predominantly Cu-N or Cu-O stretching in character, whereas the latter, with some dissent, has been attributed to a mode which is predominantly due to Cu-S stretching.[12,26d] Based upon existing data (especially recent metal isotope substitution data[59]) for nitrogeneous transition metal complexes, the assignment of the 350-450-cm^{-1} signals appears reasonable,[60] but by no means indubitable. That scattering from normal modes with large Cu-N stretching character is enhanced when the excitation is in resonance with a S → Cu charge transition can be explained by the proposal that significant displacement of the CuN_3 equilibrium geometry occurs in the charge-transfer excited state. The assignment of the 260-cm^{-1} scattering band to a Cu-S stretching mode also appears to be reasonable, in view of other work on metal-sulfur complexes,[60,61] but not completely unambiguous.

Laser Raman studies of the $[Cu^I(HB(3,5\text{-}Me_2pz)_3)(SR)]^-$, $Cu^{II}(HB(3,5\text{-}Me_2pz)_3)(SR)$, and $Cu^{II}(3,5\text{-}Me_2pz)_3)(OR)$ compounds serve four purposes. Firstly, they provide strong support for the proposed structures of the $Cu^{II}N_3(SR)$ active site analogues. Secondly, they illustrate the relationship between native and synthetic core structures. Thirdly, the Raman studies significantly strengthen the spectral assignments on the protein spectra and thus represent the beginning of a body of resonance Raman spectra-structure criteria for the blue proteins. Lastly, the spectra of the $Cu^IN_3(SR)$ derivatives provide a glimpse of what the active site in the reduced form of the blue proteins may be like and how it compares with the oxidized form in terms of force constants.

Representative laser Raman spectra are presented in Figure 7. Data are compiled in Table VII. The spectrum of **2a** was recorded in a tetrahydrofuran solution at −80 °C. Raman spectra of **1a** and **1b,** which are not resonance enhanced, could not be obtained with methanol or acetone solutions; rather, solid samples were required. Similarly, a polycrystalline sample of **3,** which does not possess the intense S → Cu charge-transfer transition at 600 nm, was used. The Raman spectrum of **2a** exhibits three polarized bands in the 385-339-cm^{-1} region and

Table VII. Position (cm^{-1}) and Assignment of Laser Raman Bands for K[Cu(HB(3,5-Me$_2$pz)$_3$)(SC$_6$H$_4$NO$_2$)]·2C$_3$H$_6$O (**1a**), K[Cu(HB(3,5-Me$_2$pz)$_3$)(SCH$_2$CH(NH$_2$)(COOC$_2$H$_5$))] (**1b**), Cu(HB(3,5-Me$_2$pz)$_3$)(SC$_6$H$_4$NO$_2$) (**2a**), and Cu(HB(3,5-Me$_2$pz)$_3$)(OC$_6$H$_4$NO$_2$) (**3**)

1a	1b	2a	3	assignment
270	275	276		ν(Cu-S)
332	335	339	311	ν(Cu-N)
351	369	360	340	ν(Cu-N)
375	399	385	369	ν(Cu-N)
			400	ν(Cu-O)

a single polarized band at 276 cm^{-1}. Except for minor differences in transition energies and intensities, the scattering patterns of **1a** and **1b** are similar to those of the cupric derivative. The Raman spectrum of **3** lacks the 270-cm^{-1} band, but displays features at 311, 340, 369, and 400 cm^{-1}. Support for the proposed structure of **2a** is derived from several lines of consideration. The observed Raman pattern is consistent with four resonance-enhanced, totally symmetric metal-ligand stretching modes expected for the CuN_3S core under distorted C_{3v} symmetry. Just such a structure has been rigorously demonstrated for **1a** and this compound (as well as **1b**) exhibits a Raman spectrum which closely corresponds to that of **2a**. That the 276-cm^{-1} signal is indeed associated with a Cu-S stretching vibration is confirmed by the results on the *p*-nitrophenolate derivative, **3**. In this case the low-frequency band is absent and a strong band is observed at 400 cm^{-1}. This feature is tentatively assigned to a mode which is largely Cu-O stretching in character.[59,60,62c,d] With the 276-cm^{-1} scattering in **2a** assigned to a Cu-S stretching vibration, the remaining three bands at 385-339 cm^{-1} are then, logically, the three expected Cu-N stretching modes, an assignment which is consistent with M-N stretching frequencies observed in other studies.[59-61,62a,b] It is significant that the cuprous and cupric $CuN_3(SR)$ derivatives exhibit similar vibrational spectra. Similarity in the structures and metal-ligand force constants should minimize inner-sphere reorganization energy (maximize Franck-Condon overlap) associated with electron transfer in both the blue proteins and synthetic analogues. Such core structures may have evolved to optimize the efficiency with which the copper ions can shuttle between oxidation states.

Electron Paramagnetic Resonance Studies. The oxidized form of the type 1 site exhibits characteristic spin Hamiltonian parameters in the range $g_\parallel \approx 2.19$-2.30 and $g_\perp \approx 2.03$-2.07 with copper hyperfine coupling constants of $A_\parallel \approx 3.3$-9.0×10^{-3} cm^{-1} and $A_\perp \approx 0$.[1-6,12] The reason for both the unusually small and unusually variable magnitude of $A_\parallel$ has evoked considerable discussion, and rationalizations based upon the nature of a copper-mercaptide bond and/or the coordination geometry of the copper ion have been invoked. EPR studies of the Cu^{II}(HB(3,5-Me$_2$pz)$_3$)(SR) and Cu^{II}(HB(3,5-Me$_2$pz)$_3$)(OR) compounds not only provide further support for the proposed structures, but allow, within the existing framework of empirical data,[13,56,63] qualitative interpretation of the structural characteristics of the blue copper binding environment.

The low-temperature EPR spectrum of **2a** in a THF glass is shown in Figure 8. Spin quantization by standard methods[64] shows that this spectrum represents 98 ± 1% of the Cu^{II} ions in the sample. Spin Hamiltonian parameters for **2a, 2b, 3,** and six blue proteins, assuming axial symmetry, are summarized in Table VIII. That the spectra of **2a** and **2b** are consistent with monomeric four-coordinate structure E is reflected in the absence of $\Delta M = 2$ (e.g., half-field) transitions, which would be indicative of dimer formation,[13,65] in the magnitudes of the spin

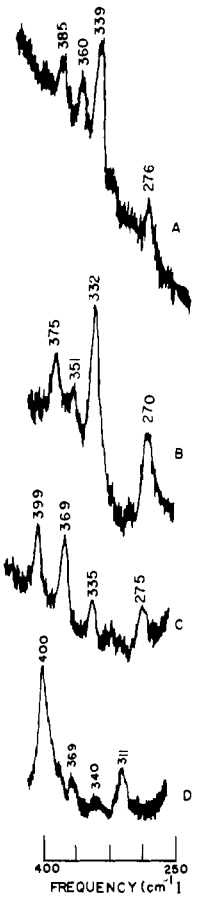

Figure 7. Raman spectra of **2a** (A) at −80 °C in THF, with Kr$^+$ (6471 Å) excitation; **1a** (B) as a solid with Ar$^+$ (5145 Å) excitation; **1b** (C) as a solid with Ar$^+$ (5145 Å) excitation; **3** (D) as a solid with Ar$^+$ (5145 Å) excitation.

Hamiltonian parameters, which are inconsistent with a five-coordinate structure,[66] and also in the presence of a seven-line superhyperfine splitting in the $g_\parallel$ direction. The superhyperfine structure indicates the presence of three-coordinated nitrogen atoms ($I = 1$), and the magnitude of A_N (0.8×10^{-3} cm^{-1}) compares favorably with the A_N observed in ENDOR studies of stellacyanin (1.2-1.6×10^{-3} cm^{-1}).[13b-d] The EPR spectrum of **3**, which represents 99 ± 1% of the Cu^{II} ions present, also exhibits no observable $\Delta M = 2$ transitions[65] and displays typical four-coordinate spin Hamiltonian parameters, and a seven-line A_N pattern is again evident in the $g_\parallel$ region. This result is consistent with structure F.

Inspection of the data in Table VIII reveals that the *g* values of **2a** and **2b** are in reasonably good agreement with those of the type 1 proteins. This is not true, however, for the $A_\parallel$ parameters, as those of the synthetic analogues are within the range of $A_\parallel$ values normally observed for Cu^{II} complexes (ca. 15-22×10^{-3} cm^{-1}), although they are at the low end of the range.[13,63,65] In considering what features of the Cu^{II} coordination environment (ligands, ligation geometry, charge) are most strongly correlated with the observed magnitudes of $g_\parallel$ and $A_\parallel$, it is worthwhile first to summarize well-documented trends, and then to examine how **2a, 2b, 3,** and the blue proteins can be accommodated within the existing framework of spectra-structure relationships.

Those factors which determine the magnitude of $g_\parallel$ in four-coordinate cupric complexes are, in decreasing order of importance, the ligands, the coordination geometry,[13f,56,67] and the overall charge of the complex.[13f] With respect to the ligand, Peisach and Blumberg[13f] as well as Addison and co-workers[56,63b] have noted that $g_\parallel$ generally decreases along the series

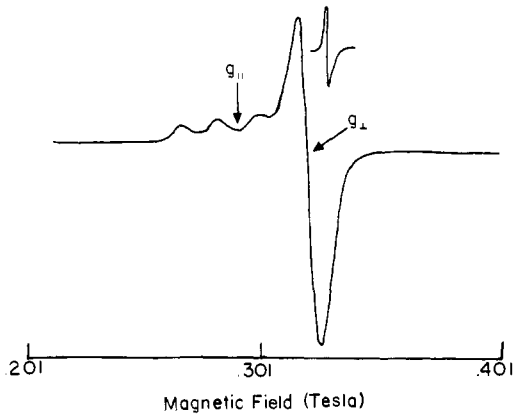

Figure 8. Electron paramagnetic resonance spectrum (9.225 GHz) of **2a** in THF glass at −196 °C. The calibrant (inset resonance) is strong pitch.

$O_4 > N_2O_2 > N_3O > N_4 > N_2S_2 > S_4$. This trend mirrors an increasing nephelauxetic[54b,68] effect, increasing covalency, and decreasing ligand electronegativity; it is in accord with theoretical calculations.[69] EPR studies on four-coordinate Cu^{II} complexes of known structure indicate that, for a given set of ligands, $g_\parallel$ increases as the coordination geometry is distorted from square planar to tetrahedral.[56a-d,63,67a] This trend has been extensively documented for $Cu^{II}N_4$, $Cu^{II}N_2O_2$, and $Cu^{II}S_4$ derivatives. The overall charge on a cupric complex has a relatively small effect on $g_\parallel$; however, Peisach and Blumberg have shown that increasing the positive charge generally increases $g_\perp$.[13f]

The relationship of $A_\parallel$ to various aspects of the Cu^{II} coordination environment is not in all cases clear. For a given set of ligands, increasing distortion of a four-coordinate copper complex from square-planar to tetrahedral geometry invariably results in a decrease in the value of $A_\parallel$.[56a,63,70] The geometry may be the single most important factor influencing this hyperfine parameter. The effect of ligands on $A_\parallel$ does not follow such a well-defined trend. Generally, substitution of an N or O donor ligand for an S donor decreases the magnitude of $A_\parallel$, providing that complex geometry and charge remain unaltered. This trend appears to mirror the nephelauxetic effect, ligand electronegativity, and bond covalency.[26d,56d,71] Generally, increasing the positive charge on a cupric compound decreases the value of $A_\parallel$.[13f] The trends in $g_\parallel$ and $A_\parallel$ with variation of ligation parameters are by no means uncorrelated. For a given set of similar ligands (e.g., N_4, N_2O_2, etc.) there is usually a linear relationship between increasing $g_\parallel$ and decreasing $A_\parallel$.[56a,62b]

To what degree do the $Cu^{II}(HB(3,5\text{-}Me_2pz)_3)(SR)$ and $Cu^{II}(HB(3,5\text{-}Me_2pz)_3)(OR)$ derivatives conform to the aforementioned spectra–structure trends? Within the series it can be seen (Table VIII) that $g_\parallel$ increases and $A_\parallel$ decreases as the variable ligand in the progression *O*-ethylcysteinate, $p\text{-}SC_6H_4NO_2$, SC_6F_5,[44] $p\text{-}OC_6H_4NO_2$ becomes increasingly electron withdrawing. This trend is as expected. Comparison of these data with EPR data for other Cu^{II} complexes is complicated by the unusual structures of the pyrazolylborate derivatives. The coordination geometries are trigonally elongated tetrahedral, which are not strictly comparable with the usually observed square-planar or D_{2d} flattened tetrahedral four-coordinate structures. Nevertheless, the $g_\parallel$ and $A_\parallel$ parameters for **2a, 2b,** and **3** fall among the literature data for cupric complexes with N_3O, N_2S_4, and N_4 ligation.[13f] Because pseudotetrahedral Cu^{II} mercaptide complexes have never before been prepared, our results provide an important observation on how such bonding affects the EPR parameters: the presence of the Cu^{II}–SR linkage does not in itself guarantee small copper hyperfine interaction.

Table VIII. EPR Data for $Cu(HB(3,5\text{-}Me_2pz)_3)(SC_6H_4NO_2)$ (**2a**), $Cu(HB(3,5\text{-}Me_2pz)_3)(SCH_2CH(NH_2)(COOC_2H_5))$ (**2b**), and $Cu(HB(3,5\text{-}Me_2pz)_3)(OC_6H_4NO_2)$ (**3**)

	$g_\parallel$	$A_\parallel \times 10^3$, cm^{-1}	$g_\perp$	ref
	Compounds			
2a	2.286	17.1	2.067	
2b	2.203	17.0	2.040	
3	2.308	16.7	2.07	
	Proteins			
Rhus vernicifera stellacyanin	2.287	3.5	2.051	13a,b,d
umecyanin	2.317	3.5	2.05	13c
Pseudomonas aeruginosa azurin	2.260	6.0	2.05	17b
spinach plastocyanin	2.226	6.3	2.053	13e
Polyporus versicolor laccase	2.19	9.0	2.03	13a,b,d
Rhus vernicifera laccase	2.23	4.3	2.05	13d

The relationship of the EPR data for **2a, 2b,** and **3** to those for blue proteins is also informative. The differences in $A_\parallel$ between **2a, 2b,** and plastocyanin, the type 1 site where ligation is most firmly established, cannot exclusively result from the specific nature of the coordinated ligands. The substitution of a thioether sulfur atom for a pyrazole group in either **2a** or **2b** should increase rather than decrease $A_\parallel$. Similarly, the difference in overall charge between the synthetic and native systems should not bring about a large difference in $A_\parallel$. On the basis of these observations we conclude that the differences in Cu^{II} coordination geometries are the principal reason for the difference in $A_\parallel$ between the blue proteins and the synthetic analogues. This conclusion is in accord with observations of other workers that sufficient distortion toward tetrahedral coordination can lower $A_\parallel$ to the "blue" region in CuN_4, CuS_4, and $CuN_2(halide)_2$ systems.[40,56a,70] The body of EPR results for low molecular weight Cu^{II} complexes highlights some significant trends in the data for the type 1 proteins. Most importantly, the wide range of protein $g_\parallel$ values, 2.19–2.31, is greater than has yet been observed for low molecular weight complexes with a constant set of coordinated ligands. It appears that no variation solely in ligation geometry can result in such a range and that appreciable differences in the ligand identities must exist among the blue proteins. As already noted, stellacyanin does not possess a methionine residue[8] and thus ligation must be different from that in plastocyanin. It is also possible that umecyanin with $g_\parallel = 2.317$ and *Polyporus versicolor* laccase with $g_\parallel = 2.19$ have ligands different from plastocyanin, and perhaps stellacyanin as well. Interestingly, in plots of $A_\parallel$ vs. $g_\parallel$, the data for the blue proteins cluster into three contiguous regions: (1) stellacyanin, umecyanin, and *R. vernicifera* laccase; (2) most azurins; (3) plastocyanins, most laccases, ascorbate oxidases, and human ceruloplasmin. This is further evidence of structural differences (ligational or geometrical) among the type 1 binding sites.

Conclusions

This study demonstrates that with the appropriate synthetic strategy it is possible to prepare and characterize $Cu^{I}N_3(SR)$ and $Cu^{II}N_3(SR)$ redox pairs which are low molecular weight approximations to proposed active sites in the blue copper proteins (structure A with X = N). These new complexes embody many of the unusual and perplexing characteristics of the type 1 core and, as such, shed considerable light on the nature of the proteins. Firstly, the 600-nm absorption, common to all of the blue copper proteins, is shown to arise from mercaptide (cysteinyl) sulfur-to-Cu charge transfer. The resonance

Raman spectra of the proteins can be assigned on the basis of metal–ligand stretches in the 350–450-cm^{-1} region and at ca. 270 cm^{-1}. The former scattering is proposed to arise from modes which are primarily Cu–N stretching in character and the latter from a mode which is largely the result of Cu–S stretching. The EPR spectra of the synthetic analogues exhibit $g_{\parallel}$ parameters that are similar to the native system. The correspondence can be understood in terms of similarities in the ligating atoms. In contrast, the copper hyperfine $A_{\parallel}$ magnitudes in the synthetic complexes do not duplicate the unusually low native values. This difference we attribute to significant differences in the Cu^{II} coordination geometries. Clearly this low hyperfine coupling is a property which is separable from the intense blue color.

The two essential characteristics of the type 1 core appear to be a unique ligand for Cu^{II}(cysteine) and a relatively unusual coordination geometry for Cu^{II}(tetrahedral or distorted tetrahedral rather than square planar or octahedral). The results on the $Cu^{II}N_3(SR)$ synthetic representations demonstrate that these two properties of the copper coordination environment are sufficient to guarantee the unique blue optical and EPR features. It is apparent that this unusual binding environment not only serves to destabilize the Cu^{II} state with respect to the Cu^{I} state, but also provides a means for "fine tuning" the protein redox potential by adjusting the coordination geometry and/or possibly the identity of the X ligand in structure A. Similarly, this unique binding environment provides a copper coordination geometry seemingly ideal for electron transfer: that with an inner sphere reorganization barrier which is not only small, but which can be adjusted by the geometry-ligation means cited above. Low molecular weight type 1 acitve site approximations offer an attractive means both to understand better the ligand and geometry sensitivity of functions such as electron transfer as well as to build a foundation of structure–spectra correlations.

Acknowledgments. We are grateful to the National Science Foundation (T.J.M., CHE76-84494A01), the Camille and Henry Dreyfus Foundation (T.J.M.), the National Institutes of Health (J.A.I., HL13157), and the National Science Foundation—MRL program through the Materials Research Center DMR76-80847 A01 of Northwestern University for generous support of this work. We thank Mr. R. C. Teitelbaum for assistance with the Raman experiments.

Supplementary Material Available: Table IV, structure amplitude table for $K[Cu(HB(3,5\text{-}Me_2pz)_3)(SC_6H_4NO_2)]\cdot 2C_3H_6O$ (5 pages). Ordering information is given on any current masthead page.

References and Notes

(1) Malkin, R. In "Inorganic Biochemistry", Vol. 2; Eichhorn, G. L., Ed.; Elsevier: Amsterdam, 1975; pp 689–709.
(2) Österberg, R. *Coord. Chem. Rev.* **1974**, *12*, 309–347.
(3) Beinert, H. *Coord. Chem. Rev.* **1977**, *15*, 119–129.
(4) Brill, A. S. "Transition Metals in Biochemistry", Springer-Verlag: New York, 1977; Chapter 3.
(5) Malkin, R.; Malmstrom, B. G. *Adv. Enzymol.* **1970**, *33*, 177–244.
(6) Fee, J. A. *Struct. Bonding (Berlin)* **1975**, *23*, 1–60.
(7) (a) Graziani, M. T.; Agro, A. F.; Rotilio, G.; Barra, O.; Mondovi, B. *Biochemistry* **1974**, *13*, 804–808. (b) Morpurgo, L.; Agro, A. F.; Rotilio, G.; Mondovi, B. *Biochim. Biophys. Acta* **1972**, *271*, 292–299.
(8) (a) Ryden, L.; Lundgren, J. O. *Nature (London)* **1976**, *261*, 344–346. (b) McLendon, G.; Martell, A. *J. Inorg. Nucl. Chem.* **1977**, *39*, 191–193. (c) Peisach, J.; Levine, W. G.; Blumberg, W. E. *J. Biol. Chem.* **1967**, *242*, 2847–2858. (d) Bergman, C.; Gandvik, E.-K.; Nyman, P. O.; Strid, L. *Biochem. Biophys. Res. Commun.* **1977**, *77*, 1052–1059. (e) Wang, T. T.; Young, N. M. *ibid.* **1974**, *74*, 119–125.
(9) (a) McMillin, D. R.; Holwerda, R. A.; Gray, H. B. *Proc. Natl. Acad. Sci. U.S.A.* **1974**, *71*, 1339–1341. (b) McMillin, D. R.; Rosenberg, R. C.; Gray, H. B. *ibid.* **1974**, *71*, 4760–4762. (c) Solomon, E. I.; Wang, R. H.; McMillin, D. R.; Gray, H. B. *Biochem. Biophys. Res. Commun.* **1976**, *69*, 1039–1042. (d) Hill, H. A. O.; Smith, B. E.; Storm, C. B.; Ambler, R. P. *ibid.* **1976**, *70*, 783–790.
(10) (a) Tennent, D. L.; Hauenstein, B. L.; McMillin, D. R. "Abstracts of Papers", 175th National Meeting of the American Chemical Society, Anaheim, Calif., March 1978; American Chemical Society: Washington, D.C., 1978; INOR 56. (b) Ferris, N. S.; Woodruff, W. H.; Tennent, D. L.; McMillin, D. R. *Biochem. Biophys. Res. Commun.* **1979**, *88*, 288–296.
(11) (a) Wherland, S.; Gray, H. B. In "Biological Aspects of Inorganic Chemistry", Addison, A. W.; Cullen, W. R.; Dolphin, D.; James, B. R., Eds.; Wiley-Interscience: New York, 1977; pp 289–368. (b) Cummins, D.; Gray, H. B. *J. Am. Chem. Soc.* **1977**, *99*, 5158–5167. (c) McArdle, J. V.; Coyle, C. L.; Gray, H. B.; Yoneda, G. S.; Holwerda, R. A. *ibid.* **1977**, *99*, 2483–2489. (d) Rosenberg, R. C.; Wherland, S.; Holwerda, R. A.; Gray, H. B. *ibid.* **1976**, *98*, 6364–6369. (e) Pecht, I.; Farver, O.; Goldberg, M. In "Bioinorganic Chemistry—II", Raymond, K. N.; Ed.; American Chemical Society: Washington, D.C., 1977; pp 179–206. (f) Gray, H. B.; Coyle, C. L.; Dooley, D. M.; Grunthaner, P. J.; Hare, J. W.; Holwerda, R. A.; McArdle, J. V.; McMillin, D. R.; Rawlings, J.; Rosenberg, R. C.; Sarlasurta, N.; Solomon, E. I.; Stephens, P. J.; Wherland, S.; Surzback, J. A. In ref 11e, pp 145–155.
(12) (a) Siiman, O.; Young, N. M.; Carey, P. R. *J. Am. Chem. Soc.* **1974**, *96*, 5583–5585. (b) *Ibid.* **1976**, *98*, 744–748. (c) Miskowski, V.; Tang, S. P.; Spiro, T. J.; Moss, T. H. *Biochemistry* **1975**, *14*, 1244–1250. (d) Tosi, L.; Garnier, A.; Herve, M.; Steinbuch, M. *Biochem. Biophys. Res. Commun.* **1975**, *65*, 100–106.
(13) (a) Vänngard, T. In "Biological Applications of Electron Spin Resonance", Swartz, H. M.; Bolton, J. R.; Borg, D. C., Eds.; Wiley: New York, 1972; Chapter 9. (b) Rist, G. H.; Hyde, J. S.; Vänngard, T., *Proc. Natl. Acad. Sci. U.S.A.* **1970**, *67*, 79–86. (c) Stigbrand, T.; Malmström, B. G.; Vänngard, T. *FEBS Lett.* **1971**, *12*, 260–262. (d) Malmström, B. G.; Reinhammar, B.; Vänngard, T. *Biochim. Biophys. Acta* **1970**, *205*, 48–57. (e) Blumberg, W. E.; Peisach, J. *ibid.* **1966**, *126*, 269–273. (f) Peisach, J.; Blumberg, J. *Arch. Biochem. Biophys.* **1974**, *165*, 691–708.
(14) (a) Peisach, J.; Mims, W. B. *Magn. Reson. Biol.*, in press. (b) Mondovi, B.; Graziani, M. T.; Mims, W. B.; Oltzik, R.; Peisach, J. *Biochemistry* **1977**, *16*, 4198–4202.
(15) (a) Markley, J. L.; Ulrich, E. L.; Krogman, D. W. *Biochem. Biophys. Res. Commun.* **1977**, *78*, 106–113. (b) Ugurbil, K.; Norton, R. S.; Allerhand, A.; Bershon, R. *Biochemistry* **1977**, *16*, 886–894. (c) Ulrich, E. L.; Markley, J. L. *Coord. Chem. Rev.* **1978**, *27*, 109–140.
(16) (a) Hill, H. A. O.; Leer, J. C.; Smith, B. E.; Storm, C. B. *Biochem. Biophys. Res. Commun.* **1976**, *70*, 331–338. (b) Markley, J. L.; Ulrich, E. L.; Berg, S. P.; Krogman, D. W. *Biochemistry* **1975**, *14*, 4428–4433. (c) Ugurbil, K.; Bersohn, R. *ibid.* **1977**, *16*, 3016–3023. (d) Surgiura, Y. *Eur. J. Biochem.* **1977**, *78*, 431–435. (e) Freeman, H. C.; Norris, V. A.; Ramshaw, J. A. M.; Wright, P. E. *FEBS Lett.* **1978**, *86*, 131–135.
(17) Hare, J. W.; Solomon, E. I.; Gray, H. B. *J. Am. Chem. Soc.* **1976**, *98*, 3205–3208.
(18) (a) Falk, K. E.; Reinhammar, B. *Biochim. Biophys. Acta* **1972**, *285*, 84–90. (b) Brill, A. S.; Bryce, G. F.; Maria, H. J. *Biochim. Biophys. Acta* **1968**, *154*, 342–351. (c) Rosen, P.; Pecht, I. *Biochemistry* **1976**, *15*, 775–786. (d) Solomon, E. I.; Hare, J. W.; Gray, H. B. *Proc. Natl. Acad. Sci. U.S.A.* **1976**, *73*, 1389–1393.
(19) (a) Solomon, E. I.; Rawlings, J.; McMillin, D. R.; Stephens, P. J.; Gray, H. B. *J. Am. Chem. Soc.* **1976**, *98*, 8046–8048. (b) Tullius, T. D.; Frank, P.; Hodgson, K. O. *ibid.* **1978**, *75*, 4069–4073.
(20) (a) Solomon, E. I.; Clendening, P. J.; Gray, H. B.; Grunthaner, F. J. *J. Am. Chem. Soc.* **1975**, *97*, 3878–3897. (b) Wurzback, J. A.; Grunthaner, P. J.; Dooley, D. M.; Gray, H. B.; Grunthaner, F. J.; Gay, R. R.; Solomon, E. I. *ibid.* **1977**, *99*, 1257–1258. (c) Peeling, J.; Haslett, B. G.; Evans, T. M.; Clark, D. T.; Boulter, D. *ibid.* **1977**, *99*, 1025–1028. (d) Larsson, S. *ibid.* **1977**, *99*, 7708–7709. (e) Best, S. A.; Brant, P.; Feltham, R. D.; Rauchfuss, T. B.; Roundhill, D. M.; Walton, R. A. *Inorg. Chem.* **1977**, *16*, 1976–1979.
(21) Gray, H. B. "Bioinorganic Chemistry", Gould, R. F., Ed.; American Chemical Society: Washington, D.C., 1971; pp 365–389.
(22) Amundsen, A. R.; Whelan, J.; Bosnich, B. *J. Am. Chem. Soc.* **1977**, *99*, 6730–6739.
(23) (a) Chapman, G. V.; Colman, P. M.; Freeman, H. C.; Guss, J. M.; Murata, M.; Norris, V. A.; Ramshaw, J. A. M.; Venkatappa, M. P. *J. Mol. Biol.* **1977**, *110*, 187–189. (b) Colman, P. M.; Freeman, H. C.; Guss, J. M.; Murata, M.; Norris, V. A.; Ramshaw, J. A. M.; Venkatappa, M. P. *Nature (London)* **1978**, *272*, 319–324. (c) Freeman, H. C. Private communication.
(24) Adman, E. T.; Stenkamp, R. E.; Sieker, L. C.; Jensen, L. H. *J. Mol. Biol.* **1978**, *123*, 35–47.
(25) (a) Sugiura, Y.; Hirayama, Y. *J. Am. Chem. Soc.* **1977**, *99*, 1581–1585. (b) Dobry-Duclaux, A.; Perichon, P. *J. Chim. Phys. Phys-Chim. Biol.* **1976**, *73*, 1058–1067. (c) Henry, Y.; Dobry-Duclaux, A. *ibid.* **1976**, *73*, 1068–1070. (d) Sugiura, Y.; Hirayama, Y. *Bioinorg. Chem.* **1978**, *9*, 521–528.
(26) (a) Jones, T. E.; Rorabacher, D. B.; Ochrymowycz, L. A. *J. Am. Chem. Soc.* **1975**, *97*, 7485–7486. (b) Miskowski, V. M.; Thich, J. A.; Solomon, R.; Schugar, H. J. *J. Am. Chem. Soc.* **1976**, *98*, 8344–8350. (c) Schugar, H. J.; Ou, C. C.; Thich, J. A.; Potenza, J. A.; Lalancette, R. A.; Furey, W. *ibid.* **1976**, *98*, 3047–3048. (d) Ferris, N. S.; Woodruff, W. H.; Rorabacher, D. B.; Jones, T. E.; Ochrymowycz, L. A. *ibid.* **1978**, *100*, 5939–5942. (e) Hughey, J. L., IV; Fawcett, T. G.; Rudich, S. M.; Lalancette, R. A.; Potenza, J. A.; Schugar, H. J. *J. Am. Chem. Soc.* **1979**, *101*, 2617–2623.
(27) (a) Thompson, J. S.; Marks, T. J.; Ibers, J. A. *Proc. Natl. Acad. Sci. U.S.A.* **1977**, *74*, 3114–3118. (b) Marks, T. J. In "Fundamental Research in Homogeneous Catalysis 2", Ishii, Y.; Tsutsui, M., Eds.; Plenum Press: New York, 1978; pp 285–300.
(28) Mealli, C.; Arcus, C. S.; Wilkinson, J. L.; Marks, T. J.; Ibers, J. A. *J. Am. Chem. Soc.* **1976**, *98*, 711–718.
(29) Thompson, J. S.; Sorrell, T.; Marks, T. J.; Ibers, J. A. *J. Am. Chem. Soc.*, following paper in this issue.
(30) (a) Trofimenko, S. *J. Am. Chem. Soc.* **1967**, *89*, 3170–3177. (b) Trofimenko, S. *Inorg. Synth.* **1970**, *12*, 99–107.
(31) Tang, S. C.; Koch, S.; Papaefthymiou, G. C.; Foner, S.; Frankel, R. B.; Ibers, J. A.; Holm, R. H. *J. Am. Chem. Soc.* **1976**, *98*, 2414–2434.
(32) Poole, C. P. "Electron Spin Resonance", Interscience: New York, 1967; pp 589–590.
(33) Doedens, R. J.; Ibers, J. A. *Inorg. Chem.* **1967**, *6*, 204–210.
(34) Those data that were initially found to have $I < 3\sigma(I)$ were rescanned with a 20-s background counting time, and the results of the two scans summed.

(35) La Placa, S. J.; Ibers, J. A. *Acta Crystallogr.* **1965**, *18*, 511–519.
(36) Cromer, D. T.; Waber, J. T. "International Tables for X-ray Crystallography", Vol. IV; Kynoch Press: Birmingham, England, 1974; Tables 2.2A and 2.3.1.
(37) See paragraph at end of paper regarding supplementary material.
(38) (a) Freeman, H. C. In "The Biochemistry of Copper", Peisach, J.; Aisen, P.; Blumberg, W. E., Eds.; Academic Press: New York, 1966; pp. 77–113. (b) Freeman, H. C. In "Inorganic Biochemistry", Vol. 1.; Eichhorn, G. L., Ed.; Elsevier: Amsterdam, 1973; pp 121–166. (c) Freeman, H. C. *Adv. Protein Chem.* **1967**, *22*, 257–424. (d) Holm, R. H.; O'Connor, M. J. *Prog. Inorg. Chem.* **1971**, *14*, 241–401. (e) Holm, R. H.; Everett, G. W.; Chakravorty, A. *ibid.* **1966**, *7*, 83–214. (f) Gazo, J.; Bersuker, I. B.; Garaj, J.; Krabesova, M.; Kohout, J.; Langfelderova, H.; Melnik, M.; Serator M.; Valach, F. *Coord. Chem.* **1976**, *19*, 253–297. (g) Buckingham, D. In ref 38b, pp 3–62. (h) Wells, A. F. "Structural Inorganic Chemistry", 3rd ed.; Oxford University Press: London, 1967; pp 856–886.
(39) (a) Maslen, H. S.; Waters, T. N. *Coord. Chem. Rev.* **1975**, *17*, 137–176. (b) Wrobleski, J. T.; Long, G. J. *Inorg. Chem.* **1977**, *16*, 2752–2762. (c) Murakami, Y.; Sakata, K. *Inorg. Chim. Acta* **1968**, *2*, 273–279. (d) Patmore, D. J.; Rendle, D. F.; Storr, A.; Trotter, J. *J. Chem. Soc., Dalton Trans.* **1975**, 718–725. (e) Johnson, J. E.; Beineke, T. A.; Jacobson, R. A. *J. Chem. Soc. A* **1971**, 1371–1374. (f) Gouge, E. M.; Geldard, J. F. *Inorg. Chem.* **1978**, *17*, 270–275. (g) Bombieri, G.; Panattoni, C.; Forsellini, E.; Graziani, R. *Acta Crystallogr., Sect. B* **1969**, *25*, 1208–1211. (h) Hall, D.; Summer, R. H.; Waters, T. N. *J. Chem. Soc. A* **1969**, 420–422. (i) Baker, E. N.; Clark, G. R.; Hall, D.; Waters, T. N. *ibid.* **1967**, 251–257. (j) Cheeseman, T. P.; Hall, D.; Waters, T. N. *ibid.* **1966**, 685–693. (k) Lingafelter, E. C.; Simmons, G. L.; Morosin, B.; Scheringer, C.; Freeberg, C. *Acta Crystallogr.* **1961**, *14*, 1222–1225. (l) Orioli, P. L.; Sacconi, L. *J. Am. Chem. Soc.* **1966**, *88*, 277–280. (m) Cheeseman, T.; Hall, D.; Waters, T. N. *Proc. Chem. Soc., London* **1963**, 379–380.
(40) Gould, D. C.; Ehrenberg, A. *Eur. J. Biochem.* **1968**, *5*, 451–455.
(41) (a) Hemmerich, P. In "The Biochemistry of Copper", Peisach, J.; Aisen, P.; Blumberg, W. E., Eds.; Academic Press: New York, 1966; pp 15–32. (b) Kroneck, P. *J. Am. Chem. Soc.* **1975**, *97*, 3839–3841. (c) Sugiura, Y.; Hirayama, Y.; Tanaka, H.; Ishizu, K. *ibid.* **1975**, *97*, 5577–5581.
(42) (a) Churchill, M. R.; DeBoer, B. G.; Rotella, F. J.; Salah, O. M. A.; Bruce, M. I. *Inorg. Chem.* **1975**, *14*, 2051–2056. (b) Bruce, M. I.; Ostazewski, A. *J. Chem. Soc., Dalton Trans.* **1973**, 2433–2436.
(43) The order and method of mixing are important. Rapid addition of SR^- to copper(II) solutions or the addition of copper(II) solutions to mercaptide solutions results in a local excess of mercaptide and, consequently, $Cu^I(SR)$ complexes.
(44) (a) The synthetic procedure described in eq 4 and 5 was used to synthesize other $Cu(HB(3,5\text{-}Me_2pz)_3)(SR)$ complexes. The complex with $SR = SC_6F_5$ was prepared in this manner and studied spectroscopically: $\lambda_{max} = 511$ nm; $g_{11} = 2.293$; $A_{11} = 16.9\ 10^{-3}\ cm^{-1}$. (b) Osborne, R. B.; Thompson, J. S.; Marks, T. J.; Ibers, J. A. Unpublished observations.
(45) Siegbahn, K.; Nordling, C.; Fahlman, A.; Nordberg, R.; Hamrin, K.; Hedman, J.; Johansson, G.; Bergmark T.; Karlsson, S.-E.; Lindgren, I.; Lindberg, B. Springfield, Va., 1968, "Electron Spectroscopy for Chemical Analysis", Technical Report AFML-TR-68-189, National Technical Information Service, pp 114–115.
(46) (a) Herting, D. L.; Sloan, C. P.; Cabral, A. W.; Krueger, J. H. *Inorg. Chem.* **1978**, *17*, 1649–1654. (b) Sloan, C. P.; Krueger, J. H. *ibid.* *1975*, *14*, 1481–1485. (c) Vitzthum, G.; Lindner, E. *Angew. Chem., Int. Ed. Engl.* **1971**, *10*, 315–326. (d) Lindner, E.; Vitzthum, G.; Langer, D.; Lorenz, I.-P. *ibid.* **1970**, *9*, 160–161.
(47) (a) Higashi, L. S.; Lundeen, M.; Hilti, E.; Seff, K. *Inorg. Chem.* **1977**, *16*, 310–313. (b) Lundeen, M.; Firor, R. L.; Seff, K. *ibid.* **1978**, *17*, 701–706.
(48) (a) Fluharty, A. L. In "The Chemistry of the Thiol Group", Part 2; Patai, S., Ed.; Wiley: New York, 1974; Chapter 13. (b) Cunningham, E. B. "Biochemistry", McGraw-Hill: New York, 1978; p 643.
(49) An explanation of the numbering system is required. C(1)–C(6), O(1), and O(2) are the atoms in the two acetone molecules. The atoms with two numbers refer to ring atoms or, in the case of the $-NO_2$ group, to atoms that are attached to a group. The first digit of the atom number designates the ring number, while the second digit designates the position in the ring. Rings 1–3 and 4 refer to the three pyrazole rings and the *p*-nitrobenzenethiolate group, respectively, which were refined as rigid bodies, with the exception of the NO_2 part.
(50) Jardine, F. H. *Adv. Inorg. Chem. Radiochem.* **1975**, *17*, 115–154.
(51) (a) Coucouvanis, D.; Hollander, F. J.; Caffery, M. L. *Inorg. Chem.* **1976**, *15*, 1853–1860. (b) Hollander, F. J.; Coucouvanis, D. *J. Am. Chem. Soc.* **1977**, *99*, 6268–6280. (c) Hollander, F. J.; Caffery, M. L.; Coucouvanis, D. *J. Am. Chem. Soc.* **1974**, *96*, 4682–4684. (d) Golding, R. M.; Rae, A. D.; Ralph, B. J.; Sulligoi, L. *Inorg. Chem.* **1974**, *13*, 2499–2504. (e) Taylor, M. R.; Glusker, J. P.; Gabe, E. J.; Minkin, J. A. *Bioinorg. Chem.* **1974**, *3*, 189–205. (f) Taylor, I. F.; Weininger, M. S.; Amma, E. L. *Inorg. Chem.* **1974**, *13*, 2835–2842. (g) Hunt, G. W.; Griffith, E. A. H.; Amma, E. L. *ibid.* **1976**, *15*, 2993–2997. (h) Weininger, M. S.; Taylor, I. F.; Amma, E. L. *Inorg. Nucl. Chem. Lett.* **1973**, *9*, 737–742. (i) Cotton, F. A.; Frenz, B. A.; Hunter, D. L.; Mester, Z. C. *Inorg. Chim. Acta* **1974**, *11*, 111–117. (j) Warner, L. G.; Otterson, T.; Seff, K. *Inorg. Chem.* **1974**, *13*, 2819–2826. (k) Ou, C. C.; Miskowski, V. M.; Lalancette, R. A.; Potenza, J. A.; Schugar, H. J. *ibid.* **1976**, *15*, 3157–3161.
(52) (a) Allman, R.; Haase, W. *Inorg. Chem.* **1976**, *15*, 804–807. (b) Washecheck, D. M.; Peterson, S. W.; Reiss, A. H.; Williams, J. M. *ibid.* **1976**, *15*, 74–78. (c) Begin, D.; Einstein, F. W. B.; Field, J. *ibid.* **1975**, *14*, 1785–1790. (d) Villa, A. C.; Manfredotti, A. G.; Giacomelli, A.; Guastini, C.; Indelli, A. *ibid.* **1975**, *14*, 1654–1658. (e) Coucouvanis, D.; Holah, D. G.; Hollander, F. J. *ibid.* **1975**, *14*, 2657–2665. (f) Hollander, F. J., Leitheiser, M.; Coucouvanis, D. *ibid.* **1977**, *16*, 1615–1619. (g) Levenson, R.; Towns, R. *ibid.* **1974**, *13*, 105–109. (h) Williams, J. M.; Keefer, K. D.; Washecheck, D. M.; Enright, N. P. *ibid.* **1976**, *15*, 2446–2455. (i) Peters, C.; Eagen, C. F. *ibid.* **1976**, *15*, 782–788. (j) Reis, A. H.; Peterson, S. W.; Washecheck, D. M.; Miller, J. S. *ibid.* **1976**, *15*, 2455–2462.
(53) (a) Williams, R. J. P. *Inorg. Chim. Acta Rev.* **1971**, *5*, 137–155. (b) Brill, A. S.; Martin, R. B.; Williams, R. J. P. In "Electronic Aspects of Biochemistry", Pullman, B., Ed.; Academic Press: New York, 1964; pp 526–530.
(54) (a) Lever, A. B. P. "Inorganic Electronic Spectroscopy", Elsevier: Amsterdam, 1968; pp 224–248. (b) Schläfer, H. L.; Glieman, G. "Basic Principles of Ligand Field Theory", Wiley-Interscience: New York, 1969; Chapter 1. (c) Barnes, J. C.; Day, P. *J. Chem. Soc.* **1964**, 3886–3892.
(55) Jørgensen, C. K. *Prog. Inorg. Chem.* **1970**, *12*, 101–158.
(56) (a) Yokoi, H.; Addison, A. W. *Inorg. Chem.* **1977**, *16*, 1341–1349. (b) Murakami, Y.; Matsuda, Y.; Sakata, K. *ibid.* **1971**, *10*, 1728–1734. (c) Yokoi, H. *Bull. Chem. Soc. Jpn.* **1974**, *47*, 3037–3040. (d) Choi, S.-N.; Bereman, R. D.; Wasson, J. R. *J. Inorg. Nucl. Chem.* **1975**, *37*, 2087–2090. (e) Yokoi, H. *Inorg. Chem.* **1978**, *17*, 538–542. (f) Wilson, R. B.; Wasson, J. R.; Hatfield, W. E.; Hodgson, D. J. *ibid.* **1978**, *17*, 641–646.
(57) (a) The 600-nm absorption exhibits substantial tailing toward long wavelength. It is conceivable that this obscures (or is in part the result of) a transition near 800 nm. (b) Cupric thioether complexes typically have an absorption in the 350–450-nm region,[22,26] but with $\epsilon \approx 3000$–$10\ 000\ M^{-1}\ cm^{-1}$. Why the corresponding protein transition is so much less intense or in a different spectral region remains an unexplained and fascinating feature of the type 1 optical spectra.
(58) (a) Spiro, T. G.; Stein, P. *Annu. Rev. Phys. Chem.* **1977**, *28*, 501–521. (b) Johnson, B. B.; Peticolas, W. L. *ibid.* **1976**, *27*, 465–492.
(59) (a) Nakamoto, K. "Infrared and Raman Spectra of Inorganic and Coordination Compounds", 3rd ed.; Wiley: New York, 1978; pp 197–370. (b) Mohan, N.; Müller, A.; Nakamoto, K. *Adv. Infrared Raman Spectrosc.* **1975**, *1*, 173–231.
(60) (a) Adams, D. M. "Metal-Ligand and Related Vibrations", St. Martin's Press: New York, 1968; pp 48–331. (b) Nakamoto, K. *Angew. Chem., Int. Ed. Engl.* **1972**, *11*, 666–674.
(61) (a) Siiman, O.; Titus, D. D.; Cowman, C. D.; Fresco, J.; Gray, H. B. *J. Am. Chem. Soc.* **1974**, *96*, 2353–2359. (b) Müller, A.; Baran, E. J.; Carter, R. O. *Struct. Bonding (Berlin)* **1976**, *26*, 81–139.
(62) (a) Marks, T. J. Unpublished Raman results on other metal pyrazolylborate complexes. This pattern is absent in $K(HB(3,5\text{-}Me_2pz)_3)$, arguing against assignment to internal ligand transitions. (b) Metal isotope substitution studies are underway. (c) Bradley, D. C.; Mehrotra, R. C.; Gaur, D. P. "Metal Alkoxides", Academic Press: New York, 1978; pp 116–122. (d) Alternatively, the Cu–O stretching mode occurs at 311 cm^{-1}.
(63) (a) Murakami, Y.; Matsuda, Y.; Sakata, K. *Inorg. Chem.* **1971**, *10*, 1734–1738. (b) Sakaguchi, U.; Addison, A. W. *J. Am. Chem. Soc.* **1977**, *99*, 5189–5190.
(64) Aasa, A.; Vanngard, T. *J. Mag. Reson.* **1975**, *19*, 308–315.
(65) (a) Smith, T. D.; Pilbrow, J. R. *Coord. Chem. Rev.* **1974**, *13*, 173. (b) Hendrickson, D. N.; Duggan, D. M. "ACS Symposium Series", No. 5; American Chemical Society: Washington, D.C., 1974, pp 76–93. (c) Hatfield, W. E. *ibid.*, pp 108–141. (d) Doumit, C. J.; McPherson, G. L.; Belford, R. L.; Lanoux, S. B.; Jonassen, H. B. *Inorg. Chem.* **1977**, *16*, 565–569. (e) Roundhill, S. G. N.; Roundhill, D. M.; Bloomquist, D. R.; Lander, C.; Willett, R. D.; Dooley, D. M.; Gray, H. B. *Inorg. Chem.*, **1979**, *18*, 831–835.
(66) Bencini, A.; Bertini, I.; Gatteschi, D.; Scozzafava, A. *Inorg. Chem.* **1978**, *17*, 3194–3197, and references cited therein.
(67) (a) Herring, F. G.; Patmore, D. J.; Storr, A. *J. Chem. Soc., Dalton Trans.* **1975**, 711–717. (b) Kivelson, D.; Neiman, R. *J. Chem. Phys.* **1961**, *35*, 149–155.
(68) Basolo, F.; Pearson, R. G. "Mechanisms in Inorganic Chemistry", 2nd ed.; Wiley: New York, 1967; p 112.
(69) Sharnoff, M. *J. Chem. Phys.* **1965**, *42*, 3383–3395.
(70) Forster, D.; Weiss, V. W. *J. Phys. Chem.* **1968**, *72*, 2669–2671.
(71) Barbucci, R.; Campbell, M. J. M. *Inorg. Chim. Acta* **1976**, *16*, 113–120.